arXiv:1404.6082v2 [hep-ph] 21 Jul 2014

Unraveling models of CP violation through electric dipole moments of light nuclei

W. Dekens[a], J. de Vries[b], J. Bsaisou[b], W. Bernreuther[c], C. Hanhart[b], Ulf-G. Meißner[b,d], A. Nogga[b], A. Wirzba[b]

[a] *University of Groningen, 9747 AA Groningen, The Netherlands*

[b] *Institute for Advanced Simulation, Institut für Kernphysik, and Jülich Center for Hadron Physics, Forschungszentrum Jülich, D-52425 Jülich, Germany*

[c] *Institut für Theoretische Physik, RWTH Aachen University, 52056 Aachen, Germany*

[d] *Helmholtz-Institut für Strahlen- und Kernphysik and Bethe Center for Theoretical Physics, Universität Bonn, D-53115 Bonn, Germany*

Abstract

We show that the proposed measurements of the electric dipole moments of light nuclei in storage rings would put strong constraints on models of flavor-diagonal CP violation. Our analysis is exemplified by a comparison of the Standard Model including the QCD theta term, the minimal left-right symmetric model, a specific version of the so-called aligned two-Higgs doublet model, and briefly the minimal supersymmetric extension of the Standard Model. By using effective field theory techniques we demonstrate to what extent measurements of the electric dipole moments of the nucleons, the deuteron, and helion could discriminate between these scenarios. We discuss how measurements of electric dipole moments of other systems relate to the light-nuclear measurements.

1 Introduction

The Standard Model (SM) of particle physics contains in the quark sector two sources of P and T violation[1]. The best understood source is the phase that is present in the three-generation quark mixing matrix, the Cabibbo-Kobayashi-Maskawa (CKM) [1,2] matrix, that induces CP-violating effects in flavor-changing processes. On the other hand, its contribution to flavor-diagonal P- and T-odd observables, such as electric dipole moments (EDMs), is highly suppressed and inaccessible with current experimental techniques. The second P- and T-violating ($\not{P}\not{T}$) source is the QCD vacuum angle $\bar{\theta}$ [3,4] which, in principle, would generate large hadronic EDMs. The null-measurement of the neutron EDM [5] strongly limits $\bar{\theta} \lesssim 10^{-10}$ [6, 7]. The puzzle of why $\bar{\theta}$ is so extremely small or perhaps zero is called the strong CP problem. In addition, it seems that both CP-odd sources in the SM are unable to account for the current matter-antimatter asymmetry in the universe [8,9]. It is therefore believed that the SM cannot be the whole story and that additional $\not{P}\not{T}$ sources exist. It has been known for a long time that searches for EDMs are highly sensitive probes of additional, flavor-diagonal CP-violating interactions. Excellent reviews on EDMs can be found in Refs. [10–12].

The above considerations have led to large experimental endeavours to measure EDMs of leptons, hadrons, nuclei, atoms, and molecules (for an overview, see Ref. [13]). At the moment the strongest existing limits have been obtained for the neutron EDM [5], the EDM of the diamagnetic ^{199}Hg atom [14], and the electron EDM (inferred from measurements on the polar molecule ThO [15]). The main motivations for this work are the plans to measure the EDMs of charged spin-carrying particles in storage rings [16–19]. The spin precession of a particle trapped in such a ring is affected by its EDM and it has been proposed that this method can be used to measure the EDMs of the proton and deuteron with a precision of $10^{-29}\,e\,$cm, three orders of magnitude better than the current neutron EDM limit. EDMs of other light ions, such as the helion (^{3}He nucleus) and triton (^{3}H nucleus) are candidates as well.

EDM experiments are very good probes for new $\not{P}\not{T}$ sources because, as mentioned, at current experimental accuracies they are 'background-free' probes of new physics. Any finite signal in one of the upcoming experiments would be due to physics not accounted for by the Kobayashi-Maskawa (KM) mechanism [2]. This source of CP violation induces only very small light quark and nucleon EDMs of the order of $10^{-31}\,e\,$cm [20,21] and even tinier lepton EDMs. A larger EDM signal might be caused by physics beyond the SM (BSM). However, it is not excluded that an extremely small, but nonzero, $\bar{\theta}$ term could be its origin. An interesting and important problem is therefore to investigate whether it is possible to trace a nonzero $\bar{\theta}$ with EDM experiments. That is, can we confidently disentangle the $\bar{\theta}$ term from possible BSM sources[2]?

To answer this question several obstacles need to be overcome. In order to separate $\bar{\theta}$ from BSM physics we need a description of the latter. Lacking knowledge of BSM physics, the only model-independent description relies on effective field theory (EFT), which requires the addition of the most general set of CP-violating higher-dimensional operators to the SM Lagrangian. The most important operators are those of dimension six (before electroweak gauge-symmetry breaking) [22, 23], while the effects of even higher-dimensional operators are expected to be suppressed. Once the set of effective dimension-six operators has been identified, it needs to be renormalization-group evolved to the low energies where the experiments take place [24–28].

[1]The models studied in this paper are CPT invariant. Therefore, P and T violation amounts to CP violation.

[2]Solely for the purpose of terminology we distinguish in this paper between the $\bar{\theta}$ term and BSM sources of CP violation. Of course, if a small but nonzero $\bar{\theta}$ exists, it may actually be generated by some BSM dynamics.

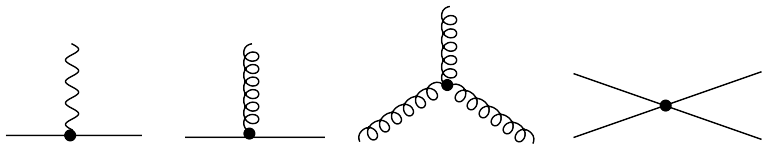

Figure 1: Schematic drawings of the $\not{P}\not{T}$ dimension-six operators in Eq. (1). The QCD $\bar{\theta}$ term is not shown. The solid, curly, and wavy lines denote external quark, gluon, and photon states respectively. The first and second diagram depict the quark EDM and chromo-EDM, respectively, the third diagram the Weinberg operator, and the fourth diagram a four-quark operator. Vertices with two or more gluon fields associated with the quark CEDM and the Weinberg operator are not shown.

The evolution of the effective operators can be calculated in perturbation theory only down to a scale Λ_χ of the order of 1 GeV. Below this scale, the expansion in the strong coupling constant breaks down and nonperturbative techniques become necessary. At the scale Λ_χ, the $\not{P}\not{T}$ low-energy effective Lagrangian of the quark and gluon degrees of freedom schematically takes on the form (see also Fig. 1):

$$\begin{aligned}\mathcal{L}_{\not{P}\not{T}} &= -\bar{\theta}\frac{g^2}{64\pi^2}\epsilon^{\mu\nu\alpha\beta}G^a_{\mu\nu}G^a_{\alpha\beta} - \frac{1}{2}\sum_{q=u,d}\left(d_q\,\bar{q}i\sigma^{\mu\nu}\gamma_5 q\,F_{\mu\nu} + \tilde{d}_q\,\bar{q}i\sigma^{\mu\nu}\gamma_5 t_a q\,G^a_{\mu\nu}\right)\\ &\quad + \frac{d_W}{6}f_{abc}\varepsilon^{\mu\nu\alpha\beta}G^a_{\alpha\beta}G^b_{\mu\rho}G^{c\,\rho}_{\nu} + \sum_{i,j,k,l=u,d}C_{ijkl}\,\bar{q}_i\Gamma q_j\,\bar{q}_k\Gamma' q_l\ , \end{aligned} \tag{1}$$

in terms of the quark fields q, the photon and gluon field-strength tensors $F_{\mu\nu}$ and $G^a_{\mu\nu}$, respectively. The f_{abc} are the structure constants and the t_a are the generators in the fundamental representation of $SU(3)_c$. The coefficients d_q and $\tilde{d}_q$ are the electric dipole and chromo-electric dipole moments (CEDM) of quarks, and the coefficient d_W of the Weinberg operator [29] can be interpreted as the chromo-electric dipole moment (gCEDM) of the gluon [25,30]. The last term contains four-quark operators with zero net-flavor where the matrices Γ and Γ' denote various Lorentz structures such that the four-quark operators violate the CP symmetry. In this work, we consider the low-energy $\not{P}\not{T}$ Lagrangian for u and d valence quarks only, which is appropriate for analyzing the EDMs of nucleons and light nuclei. The first operator in Eq. (1) is the dimension-four QCD $\bar{\theta}$ term, while the others are or arise from dimension-six operators (before electroweak gauge-symmetry breaking) and are generated by BSM dynamics. The second and third operators are the quark EDMs and chromo-EDMs respectively, the fourth operator is the Weinberg operator [29], and the last term denotes various $\not{P}\not{T}$ four-quark operators. We will discuss these operators in much more detail in the subsequent sections.

Below the scale Λ_χ, EFTs are again a very powerful tool in understanding low-energy strong interactions. By constructing the most general interactions for the low-energy degrees of freedom which are consistent with the symmetries of QCD, chiral symmetry in particular, and with their spontaneous and explicit breakdown, it is possible to obtain an effective low-energy description of QCD called chiral perturbation theory (χPT) [31–35]. The main advantage of χPT is that observables can be calculated perturbatively with an expansion parameter q/Λ_χ where q is the typical momentum scale of the process under consideration. Each interaction appearing in the chiral Lagrangian is associated with a low-energy constant (LEC) whose size is not fixed by symmetry considerations and depends on the strong nonperturbative dynamics. However, the

perturbative nature of χPT ensures that most observables only depend on a small number of LECs. Once these LECs have been determined, either by fitting them to data or by direct lattice calculations, other observables can be firmly predicted. Another major success of χPT is the description of the nucleon-nucleon and multi-nucleon interactions. This has opened up the way to describe nucleons and (light) nuclei in a unified framework [36–38].

In recent years, χPT has been extended to include effects of the $\bar{\theta}$ term [39] and $\not{P}\not{T}$ BSM operators up to dimension-six [40] which induce $\not{P}\not{T}$ interactions in the chiral Lagrangian. The so-amended χPT allows for the calculation of the EDMs of the nucleon [41–48] and light nuclei [49–51] in terms of the various LECs associated with the $\not{P}\not{T}$ chiral interactions. The nuclear uncertainties can be quantified and improved upon systematically. Although the hadronic uncertainty in the sizes of the LECs themselves is sizable, the same LECs appear in several EDMs which means that the hadronic uncertainties cancel to a large degree. It is this property, in addition to the high envisaged experimental accuracy, which makes the plans to measure the EDMs of light nuclei so exciting. Calculations of EDMs of heavier systems, such as ^{199}Hg, suffer from much larger nuclear uncertainties which are hard to quantify [12, 52].

Although the $\bar{\theta}$ term and the higher-dimensional operators in Eq. (1) all break P and T, they transform differently under chiral and isospin rotations. This ensures that the different $\not{P}\not{T}$ sources induce different $\not{P}\not{T}$ chiral Lagrangians, which, in turn, lead to distinct patterns of EDMs. This observation has been used in recent works which concluded that it is possible to disentangle the $\bar{\theta}$ term from the higher-dimensional BSM operators, given enough EDM measurements [49–51, 53]. In particular, the EDM of the deuteron plays an important role. Furthermore, several classes of dimension-six operators can be disentangled among themselves as well. Again the deuteron EDM plays an important role, but the EDMs of the helion and/or triton give important complementary information.

The investigation of light-nuclear EDMs so far has focused mainly on the $\bar{\theta}$ term and dimension-six operators individually. That is, it was assumed [40,49–51] that one operator is dominant over the others which has the advantage of a rather clean analysis. It can be questioned, however, how realistic such a scenario is. It could very well be that the underlying microscopic theory induces contributions of similar size to several effective dimension-six operators. Furthermore, even if only one operator turns out to be dominant at high energies, this operator can induce sizable contributions to other operators when evolved to the low-energy scale where EDM experiments take place. Therefore, the assumption of one dominant dimension-six operator at low energies might not be the most likely one. To investigate this in more detail, we study in this work four distinct scenarios of non-KM *CP* violation and investigate whether EDM measurements can discriminate between them. However, the methods used are in no way limited to these four scenarios and can be easily applied to other BSM models.

In the first scenario we assume the SM $\bar{\theta}$ term to be the dominant source. Since, with the exception of the CKM matrix, this is the only *CP*-violating term of dimension four in the hadronic sector, it provides the background to which the other scenarios, which induce $\not{P}\not{T}$ operators with dimension of at least of dimension six, have to be compared to. The $\bar{\theta}$ scenario has already been studied extensively in the literature (although we will consider here some very recent results on light-nuclear EDMs [54, 55]) and we will mainly summarize the results in the following. For the BSM models discussed in this paper, we assume that the $\bar{\theta}$ term is absent, for instance, due to a Peccei-Quinn symmetry [56, 57] of the Lagrangian of the respective model.

The second scenario is the minimal left-right symmetric model [58–60]. In this model, parity is restored at energies above the electroweak scale by extending the SM gauge symmetry to

include $SU(2)_R$. It turns out that in this model the dominant contribution to the respective $\not{P}\not{T}$ Lagrangian at high energies is due to one particular dimension-six operator. This operator mixes with only one additional operator such that the low-energy Lagrangian at the quark level is rather simple. However, these operators transform in a rather complicated way under chiral symmetry. As a result, the induced chiral Lagrangian contains some interesting and nontrivial structures. These structures induce a profound hierarchy of nuclear EDMs which is quite distinct from the $\bar{\theta}$ scenario.

The third scenario we investigate is based on the so-called aligned two-Higgs-doublet model (a2HDM) [61]. Contrary to the two scenarios just outlined, in this model, which exemplifies the generic feature of non-KM *CP* violation in two-Higgs doublet-models, several $\not{P}\not{T}$ operators are induced at the level of quarks and gluons which, in general, make contributions of comparable size to hadronic EDMs. The coefficients of these operators depend on different parameters of the model. The main goal of this work to show that the EDMs of nucleons and light nuclei can be used to disentangle different scenarios, and we do not aim at a fully detailed analysis of the a2HDM. We therefore make certain assumptions [62] regarding the neutral Higgs sector such that all induced higher-dimensional BSM operators depend on the same combination of parameters. Despite this simplification, the EDMs of nucleons and light nuclei receive comparable contributions from three BSM operators which makes the analysis more complicated and uncertain. Nevertheless, we demonstrate that the model still leads to a different hierarchy of EDMs than the previous scenarios.

Furthermore, we shortly discuss another popular BSM model with non-KM *CP* violation, the minimal supersymmetric extension (MSSM) of the Standard Model. Also in this model, the contribution to the hadronic EDMs is, in general, not dominated by just one $\not{P}\not{T}$ operator at the level of quarks and gluons.

We will show that estimates of the nucleon EDMs alone are insufficient to disentangle these scenarios. In fact, the predictions and estimates of the two-nucleon contribution to the EDMs of the light ions, especially of the deuteron and helion, will be crucial in disentangling the various sources. The measurements of the deuteron and helion EDM provide in this regard 'orthogonal' information, because the isospin-filter property of the deuteron favors isospin-breaking interactions, while the helion allows for both isospin-conserving and -breaking contributions.

This article is organized as follows. In Sect. 2 we discuss the four different scenarios of *CP* violation outlined above. In particular we focus on the low-energy $\not{P}\not{T}$ interactions that are induced in these scenarios. In Sect. 3 we discuss the most important $\not{P}\not{T}$ hadronic interactions that appear in each of the scenarios. In particular we focus on the $\not{P}\not{T}$ pion-nucleon interactions and the nucleon EDMs. In Sect. 4 we turn to the EDMs of light nuclei. We argue that chiral effective field theory is a powerful tool to study these observables and show that measurements of light-nuclear EDMs can be used to disentangle different scenarios. In Sect. 5 we briefly discuss other systems, in particular the EDMs of the electron and the diamagnetic atom ^{199}Hg. We summarize, conclude, and give an outlook in Sect. 6. Several appendices are devoted to technical details.

2 Four scenarios of CP violation

In this section we discuss in detail four distinct scenarios of *CP* violation. In particular we discuss the low-energy $\not{P}\not{T}$ operators that are induced in each scenario. In this work we mainly

focus on the EDMs of nucleons and light nuclei. Therefore we concentrate here on the $\not{P}\not{T}$ operators involving quark and/or gluon fields, while (semi-)leptonic operators are discussed in Sect. 5.

2.1 The QCD $\bar{\theta}$ term

The QCD Lagrangian for two quark flavors is given by

$$\mathcal{L}_{\rm QCD} = -\frac{1}{4} G^a_{\mu\nu} G^{a,\mu\nu} + \bar{q}(i\not{D} - M)q - \bar{\theta}\frac{g^2}{64\pi^2}\epsilon^{\mu\nu\alpha\beta} G^a_{\mu\nu} G^a_{\alpha\beta} \ , \tag{2}$$

where $q = (u\,, d)^T$ denotes the quark doublet of up and down quarks. As already mentioned above, the restriction to two quark flavors is appropriate for analyzing the EDMs of nucleons and light nuclei within the framework of χPT. In Eq. (2) $G^a_{\mu\nu}$ is the gluon field strength tensor, $\epsilon^{\mu\nu\alpha\beta}$ ($\epsilon^{0123} = +1$) is the completely antisymmetric tensor in four dimensions, D_μ the gauge-covariant derivative, M the real-valued quark 2×2 mass matrix, and $\bar{\theta}$ the coupling constant of the so-called $\bar{\theta}$ term which violates P and T. In this expression, we have absorbed the complex phase of the quark mass matrix into $\bar{\theta} = \theta + \arg\det(M)$. Due to the $U_A(1)$ anomaly, an axial $U(1)$ transformation of the quark fields can be used to remove the $\bar{\theta}$ term from the Lagrangian. After vacuum alignment [6] and assuming $\bar{\theta} \ll 1$, the QCD Lagrangian becomes

$$\mathcal{L}_{QCD} = -\frac{1}{4} G^a_{\mu\nu} G^{a,\mu\nu} + \bar{q} i\not{D} q - \bar{m}\bar{q}q - \varepsilon\bar{m}\bar{q}\tau_3 q + m_*\bar{\theta}\bar{q}i\gamma^5 q \ , \tag{3}$$

in terms of the averaged quark mass $\bar{m} = (m_u + m_d)/2$ in the two-flavor case, the quark-mass difference $\varepsilon = (m_u - m_d)/(m_u + m_d)$, and the reduced quark mass $m_* = m_u m_d/(m_u + m_d) = \bar{m}(1-\varepsilon^2)/2$. This expression shows that $\not{P}\not{T}$ effects due to the $\bar{\theta}$ term would vanish if one of the quarks were massless. However, this is not realized in nature [63]. We also give the explicit PT-even quark mass terms here because, as we will discuss later, $\not{P}\not{T}$ hadronic interactions induced by the $\bar{\theta}$ term are closely linked to PT-even isospin-breaking interactions induced by the quark mass difference.

Before continuing the analysis of the $\bar{\theta}$ term, we first discuss the BSM scenarios used in this paper. In these scenarios we assume that the $\bar{\theta}$ term is absent, for example, due to the Peccei-Quinn mechanism [56, 57] or by extreme fine-tuning. It should be noted that the Peccei-Quinn mechanism would, apart from removing the $\bar{\theta}$ term, also affect the dimension-six operators appearing in the other scenarios [11].

2.2 The minimal left-right symmetric model

Left-right symmetric (LR) models are based on the gauge group $SU(3)_c \times SU(2)_L \times SU(2)_R \times U(1)_{B-L}$ with an unbroken parity symmetry at high energies [58, 59, 64–66]. The abelian subgroup is associated with baryon minus lepton number. The left-handed and right-handed quarks and leptons form fundamental representations of $SU(2)_L$ and $SU(2)_R$, respectively. As a con-

sequence, right-handed neutrinos are introduced automatically:

$$\begin{aligned} Q_L &= \begin{pmatrix} U_L \\ D_L \end{pmatrix} \in (3,2,1,1/3)\ , \qquad Q_R = \begin{pmatrix} U_R \\ D_R \end{pmatrix} \in (3,1,2,1/3)\ , \\ L_L &= \begin{pmatrix} \nu_L \\ l_L \end{pmatrix} \in (1,2,1,-1)\ , \qquad L_R = \begin{pmatrix} \nu_R \\ l_R \end{pmatrix} \in (1,1,2,-1)\ , \end{aligned} \tag{4}$$

where the capital letters Q, U, D, and L denote quarks or leptons of any generation. Given the fermion assignment, at least one spin-zero bidoublet, ϕ, with the assignment $(1,2,2,0)$, is needed to generate fermion masses. The LR model is called *minimal* [60] if just one bidoublet is used such that the model is parity-invariant before gauge-symmetry breaking, but *CP* is broken both explicitely and spontaneously.

At some high-energy scale above the electroweak scale the extended gauge-group of the LR model should be broken down to the SM gauge-group. In order to achieve this, additional spin-zero fields are employed. In the version of the minimal LR model (mLRSM) we will discuss here, *cf.* [60,66], this is done with two triplets $\Delta_{L,R}$ belonging to $(1,3,1,2)$ and $(1,1,3,2)$, respectively. The spin-zero fields can be written in the form

$$\phi = \begin{pmatrix} \phi_1^0 & \phi_2^+ \\ \phi_1^- & \phi_2^0 \end{pmatrix}, \qquad \Delta_{L,R} = \begin{pmatrix} \delta_{L,R}^+/\sqrt{2} & \delta_{L,R}^{++} \\ \delta_{L,R}^0 & -\delta_{L,R}^+/\sqrt{2} \end{pmatrix}\ . \tag{5}$$

With this definition of the fields the parity transformation is equivalent to changing the (L, R) indices of all fields to (R, L) and letting $\phi \to \phi^\dagger$. Among other things this symmetry implies that the coupling constants of the two $SU(2)$ gauge-groups are equal.

In order to achieve the breaking of both the gauge symmetries and the parity symmetry, the neutral components of the spin-zero fields are assumed to acquire vacuum expectation values (vevs). First, the symmetry group $SU(3)_c \times SU(2)_L \times SU(2)_R \times U(1)_{B-L}$ is broken to down to the SM gauge group, $SU(3)_c \times SU(2)_L \times U(1)_Y$ by the vev $\langle \Delta_R \rangle = v_R$ at a scale of several TeV. This gauge-symmetry breaking entails also the breaking of the parity symmetry. The vev v_R sets the scale of the masses of the additional gauge bosons, $W_R^\pm$ and Z_R, of the $SU(2)_R$ gauge group. In order for the mLRSM to satisfy the experimental bounds coming from K- and B-meson mixing, the mass of the right-handed $W_R^\pm$ boson is constrained to $M_{W_R} \geq 3.1\,\text{TeV}$ [67]. At lower energies, electroweak symmetry breaking is achieved by the vevs of the bidoublet ϕ. Lastly, the vev $\langle \Delta_L \rangle = v_L$ gives rise to a Majorana mass term for the left-handed neutrinos. This implies that this vev should not be much larger than the scale of the neutrino mass, $v_L \lesssim \mathcal{O}(\text{eV})$. The vev v_L and its phase θ_L, however, do not enter in the terms in the Lagrangian in Eq. (1) which are important for hadronic EDMs. Therefore, they will not play a role in any of our calculations below. Explicitly, the spin-zero fields acquire the following vacuum expectation values with two observable *CP*-violating phases, which by convention, are put into the vev of the second doublet and of Δ_L [60, 66]:

$$\langle \phi \rangle = \begin{pmatrix} \kappa & 0 \\ 0 & \kappa' e^{i\alpha} \end{pmatrix}\ , \qquad \langle \Delta_L \rangle = \begin{pmatrix} 0 & 0 \\ v_L e^{i\theta_L} & 0 \end{pmatrix}\ , \qquad \langle \Delta_R \rangle = \begin{pmatrix} 0 & 0 \\ v_R & 0 \end{pmatrix}\ . \tag{6}$$

The vevs κ, κ' set the scale of the masses of the $W_L^\pm$ and Z_L gauge bosons of the $SU(2)_L$ gauge group. We have

$$\sqrt{2}\sqrt{\kappa^2 + \kappa'^2} = v \simeq 246\,\text{GeV} \ . \tag{7}$$

CP violation in the quark sector of the mLRSM arises from a number of phases. From explicit and spontaneous *CP* breaking in the Higgs potential, the *CP*-violating phase α of Eq. (6) is generated [66]. Secondly, additional phases will appear in the quark mixing matrices V_L and V_R. The matrix V_L of the left-handed quarks, which is identical to the CKM matrix of the SM, contains one observable phase. Similarly, a right-handed analogue of the CKM matrix is produced when the quark mass-eigenstates are not aligned with the $SU(2)_R$ eigenstates, which will be the case in general. In addition to the KM phase in V_L, there are then six additional phases in V_R. However, in order to produce the correct pattern of quark masses the model parameters have to be tuned in such a way that there is an approximate relation between the two quark mixing matrices and their phases [68].

Having discussed the model we are now ready to integrate out the heavy fields and derive the dimension-six *CP*-odd operators produced at the electroweak scale that are relevant for the effective Lagrangian in Eq. (1). The phases in V_L and V_R, together with the phase α, produce a number of *CP*-violating operators at the electroweak scale. However, just one of these operators is generated at tree level, while the others are induced at the one-loop level. Hadronic EDMs in the mLRSM are therefore dominated by this single operator. For a more detailed discussion we refer to Appendix A and Refs. [69, 70]. Below the scale of the new physics, this dominant interaction takes the form of the following gauge-invariant Lagrangian [23, 71],

$$\mathcal{L}_{LR}\big|_{\mu \lesssim v_R} = \Xi_1 (i\tilde{\varphi}^\dagger D_\mu \varphi)(\overline{u}_R \gamma^\mu d_R) + \text{h.c.} \ , \qquad \Xi_1 = \frac{2}{v^2}\frac{\kappa\kappa'}{v_R^2} V_R^{ud} e^{i\alpha} \simeq -\frac{2}{v^2}\sin\zeta\, V_R^{ud} e^{i\alpha} \ , \tag{8}$$

where φ corresponds to the SM Higgs-doublet (see Appendix A), $\tilde{\varphi} = i\tau_2\varphi^*$, and $\mu \lesssim v_R$ indicates the scale where the above effective Lagrangian describes the dominant *CP* violation in this model. Furthermore, $\sin\zeta \simeq -\kappa\kappa'/v_R^2$ is the angle describing the mixing between the $W_L^\pm$ and $W_R^\pm$ bosons, see, for instance, Ref. [60]. After electroweak symmetry breaking, this operator becomes in the unitary gauge

$$\mathcal{L}_{LR}\big|_{\mu \sim v} = -\frac{g v^2}{2\sqrt{2}}\left[\Xi_1\, \overline{u}_R \gamma^\mu d_R W_{L\mu}^+ + \text{h.c.}\right]\left(1 + \frac{h}{v}\right)^2 \ , \tag{9}$$

where h is the lightest Higgs boson of the model, i.e., it corresponds to the 126 GeV spin-zero resonance discovered at the LHC [72, 73].

The above interaction is essentially a coupling of the $W_L^\pm$ boson to right-handed quarks. This interaction is generated because both $W_L^\pm$ and $W_R^\pm$ interact with the bidoublet ϕ, as this field is charged under $SU(2)_L$ and $SU(2)_R$. Through their interactions with the bidoublet, $W_L^\pm$ and $W_R^\pm$ effectively mix among each other. Thus, after integrating out the heavy $W_R^\pm$ boson, the remaining $W_L^\pm$ boson obtains a (small) coupling to right-handed fields in the form of the operator in Eq. (9).

The operator in Eq. (8) remains invariant under QCD renormalization-group evolution. Therefore we can trivially lower the energy to the electroweak scale. In order to move to even lower energies, we need to integrate out the heavy SM fields. Integrating out the $W_L^\pm$ and Higgs

fields, we obtain, just below the mass of the $W_L^\pm$ boson,

$$\mathcal{L}_{LR}\big|_{\mu\lesssim m_W} = -i\,\mathrm{Im}\left(V_L^{ud*}\,\Xi_1(M_W)\right)\left(\overline{u}_R\gamma^\mu d_R\,\overline{d}_L\gamma_\mu u_L - \overline{d}_R\gamma^\mu u_R\,\overline{u}_L\gamma_\mu d_L\right) + \dots \ , \tag{10}$$

where the dots denote suppressed operators. The resulting four-quark operator is affected by QCD corrections and, in fact, mixes with a second operator which has the same Lorentz but different color structure. At a scale where perturbative QCD is still valid, well above the chiral scale $\Lambda_\chi \sim 1\,\mathrm{GeV}$, we obtain,

$$\begin{aligned}\mathcal{L}_{LR}\big|_{\mu\sim\Lambda_\chi} \ = \ & -i\eta_1\,\mathrm{Im}\left(V_L^{ud*}\,\Xi_1(M_W)\right)\left(\overline{u}_R\gamma^\mu d_R\,\overline{d}_L\gamma_\mu u_L - \overline{d}_R\gamma^\mu u_R\,\overline{u}_L\gamma_\mu d_L\right) \\ & -i\eta_8\,\mathrm{Im}\left(V_L^{ud*}\,\Xi_1(M_W)\right)\left(\bar{u}_R\gamma^\mu t_a d_R\,\bar{d}_L\gamma_\mu t_a u_L - \bar{d}_R\gamma^\mu t_a u_R\,\bar{u}_L\gamma_\mu t_a d_L\right) + \dots \ ,\end{aligned} \tag{11}$$

where $\eta_1 = 1.1$ and $\eta_8 = 1.4$ are factors appearing due to QCD evolution [28]. As these four-quark operators contribute to hadronic EDMs, their coefficients can be bounded by the upper limit on the neutron EDM. This gives $v^2\mathrm{Im}\left(V_L^{ud*}\,\Xi_1(M_W)\right) \leq 8\cdot 10^{-5}$, see Sect. 6.2. A stronger bound was found in Ref. [60], but a a recent χPT analysis indicated that the strength of this upper bound has been overestimated [74]. In any case, in the mLRSM, the dominant *CP*-violating contribution to the effective Lagrangian in Eq. (1) at the chiral scale is given by the combination of four-quark operators in Eq. (11).

2.3 The aligned two-Higgs-doublet model

Two-Higgs-doublet models (2HDMs) are among the simplest extensions of the SM. Among other features they provide an interesting source for non-KM *CP* violation, namely *CP* violation induced by neutral and charged Higgs boson exchange, for reviews, see, e.g., Refs. [75–77]. In these models the SM field content is extended by an additional Higgs doublet. There are thus two doublets, Φ_1 and Φ_2, both transforming under $SU(3)_c \times SU(2)_L \times U(1)_Y$ as $(1, 2, 1/2)$. The electroweak symmetry is broken by the vevs of the neutral components of Φ_1 and Φ_2. One can always choose a so-called Higgs basis (see, for instance, Ref. [77]), in which only one of the doublets acquires a vev,

$$\langle\Phi_1\rangle = (0, v/\sqrt{2})^T \ , \qquad \langle\Phi_2\rangle = 0 \ , \tag{12}$$

where $v = \sqrt{v_1^2 + v_2^2} \simeq 246\,\mathrm{GeV}$. In this basis the would-be Goldstone boson fields G^0 and G^+ are contained in Φ_1:

$$\Phi_1 = \begin{pmatrix} G^+ \\ (v + S_1 + iG^0)/\sqrt{2}\end{pmatrix} \ , \qquad \Phi_2 = \begin{pmatrix} H^+ \\ (S_2 + iS_3)/\sqrt{2}\end{pmatrix} \ . \tag{13}$$

Thus, the physical spin-zero fields of the 2HDM consist of 3 neutral fields, $S_{1,2,3}$, and one charged field, H^+. The neutral fields in the mass basis, $\varphi_1^0, \varphi_2^0, \varphi_3^0$, are linear combinations of the fields S_i. The two sets of fields are related by an orthogonal 3×3 matrix R, $\varphi_i^0 = R_{ij}S_j$. In general, the Higgs potential of a 2HDM violates *CP*. As a consequence, the φ_i^0 do not have a definite *CP* parity. The lightest of the fields φ_i^0 corresponds to the 126 GeV spin-zero resonance discovered at the LHC [72,73]. If the Higgs potential conserves *CP*, then two of the φ_i^0 have *CP* parity $+1$, while the third one has *CP* parity -1. In this case, the fields in the mass basis are traditionally

denoted by h, H, A, where h describes the lightest of the two scalar states. For the sake of simplicity, we shall use here the notation $(\varphi_i^0) = (h,\, H,\, A)$ also in the case of Higgs sector CP violation, when h, H, and A no longer have a definite CP parity.

The most important contributions to EDMs arise from the interactions of the spin-zero fields with fermions. The most general Yukawa Lagrangian in the quark sector that obeys the SM gauge symmetries is given by

$$-\mathcal{L}_{Y'} = \frac{\sqrt{2}}{v}\left[\bar{Q}'_L(M'_d\Phi_1 + Y'_d\Phi_2)D'_R + \bar{Q}'_L(M'_u\tilde{\Phi}_1 + Y'_u\tilde{\Phi}_2)U'_R + \text{h.c.}\right] \ . \tag{14}$$

Here Q'_L, U'_R, and D'_R denote the $SU(2)_L$ quark doublet and singlets, respectively, in the weak-interaction basis, $M'_{u,d}$ and $Y'_{u,d}$ are complex 3×3 matrices; $M'_{u,d}$ are the quark mass matrices to which $Y'_{u,d}$, in view of having chosen the Higgs basis, do not contribute.

So far we have discussed a general 2HDM. The requirement for restricting these models comes from the fact that in its general form the 2HDM generates tree-level flavor-changing neutral-currents (FCNCs) [75–77]. One way to make sure these tree-level FCNCs are absent is to impose a Z_2 symmetry on the model which may be softly broken by the Higgs potential [75–77]. An alternative and more general way is to assume that the matrices M'_q and Y'_q $(q = u, d)$ are, at some (high) scale, proportional to each other and can therefore be simultaneously diagonalized [61]:

$$Y_d = \varsigma_d M_d \ , \qquad Y_u = \varsigma_u^* M_u \ , \tag{15}$$

where $M_{u,d}$ are the real diagonal quark mass matrices and ς_u and ς_d are complex numbers. The model using this assumption is called the aligned two-Higgs doublet model (a2HDM) [61]. This is similar to the hypothesis of 'minimal flavor violation' [78–80].

In the mass basis both for the quark and the Higgs fields, one obtains from Eq. (14), using Eq. (15), the Yukawa interactions of the quark and the physical Higgs fields $H^\pm$ and φ_i^0:

$$\begin{aligned} -\mathcal{L}_Y &= \frac{\sqrt{2}}{v}H^+\bar{U}\left[\varsigma_d V M_d\mathcal{P}_R - \varsigma_u M_u V\mathcal{P}_L\right]D \\ &+ \frac{1}{v}\sum_{i=1}^{3}\left[y_u^i\varphi_i^0\,\bar{U}_L M_u U_R + y_d^i\varphi_i^0\,\bar{D}_L M_d D_R\right] + \text{h.c.} \quad , \end{aligned} \tag{16}$$

where V is the CKM matrix and $\mathcal{P}_{R,L} = (1 \pm \gamma_5)/2$. The reduced Yukawa couplings y_u^i and y_d^i of the neutral Higgs bosons are given in terms of the complex parameters $\varsigma_{u,d}$ and the matrix elements of the 3×3 real orthogonal Higgs mixing matrix R (see above) by [61]:

$$y_u^i = R_{i1} + (R_{i2} - iR_{i3})\varsigma_u^* \ , \tag{17}$$

$$y_d^i = R_{i1} + (R_{i2} + iR_{i3})\varsigma_d \ . \tag{18}$$

The orthogonality of R implies

$$\sum_{i=1}^{3}\text{Re}\, y_q^i\,\text{Im}\, y_{q'}^i = r_{q'}\text{Im}\,(\varsigma_q^*\varsigma_{q'}) \ , \tag{19}$$

where $r_u = -1$, $r_d = 1$. The Yukawa couplings to leptons are analogous to those of the down-type quarks. Resulting CP-violating effects involving leptons effects will be commented on in Sect. 5.1 and in Appendix B.

The interactions in Eq. (16) and the couplings in Eqs. (17) and (18) exhibit several interesting features. a) The exchange of a charged Higgs boson between quarks transports, apart from the KM-phase that plays no role in the discussion below, also the *CP*-violating phases of $\varsigma_{u,d}$. These phases induce, for instance, flavor-diagonal *CP*-odd four-quark operators already at tree-level of the type $(\bar{u}d)(\bar{d}i\gamma_5 u)$, where u (d) denotes any of the up-type (down-type) quarks, with operator coefficients proportional to $\mathrm{Im}(\varsigma_u^*\varsigma_d)$. b) If the Higgs potential violates *CP*, the neutral Higgs states are, as mentioned, no longer *CP* eigenstates and their exchange induces, for instance, flavor-diagonal *CP*-odd four-quark operators $(\bar{q}q)(\bar{q}'i\gamma_5 q')$, $(q, q' = u, d)$ at tree level, in particular the operators $(\bar{q}q)(\bar{q}i\gamma_5 q)$. c) If the (tree level) Higgs potential of the a2HDM is *CP*-invariant, neutral Higgs exchange nevertheless induces *CP*-odd operators of the type $(\bar{u}u)(\bar{d}i\gamma_5 d)$ if $\mathrm{Im}(\varsigma_u^*\varsigma_d) \neq 0$. Features a) and c) distinguish the a2HDM from 2HDM with a Z_2 symmetry that is (softly) broken by *CP*-violating Higgs potential, *cf.*, for instance Ref. [81,82].

As already mentioned above, the lightest neutral Higgs boson h is to be identified with the 126 GeV spin-zero boson discovered at the LHC. The experimental analysis of this resonance does not (yet) prove that it is a pure scalar, but the data indicate [83,84] that a possible pseudoscalar component of this state must be smaller than the scalar one. Therefore, we make the following simplifying assumptions:

$$\begin{aligned} &(i) \qquad R_{11} \to 1 \ , \qquad R_{12} \to 0 \ , \qquad R_{13} \to 0 \ , \\ &(ii) \qquad M_H \to M \ , \qquad M_A \to M \ . \end{aligned} \tag{20}$$

Assumption (i) amounts to assuming that the lightest Higgs boson h is a pure scalar[3], while with (ii) we assume that the two heavier neutral Higgs bosons H and A are (nearly) mass-degenerate. These assumptions are not meant to single out a particular phenomenologically or theoretically favored version of the a2HDM. They just serve to simplify the dependence of the quark and gluon (C)EDMs on unknown parameters of the model. In this way their sizes can be compared.

We can now construct the relevant *CP*-violating operators up to dimension-six that are generated at a high scale $\mu \sim$ a few hundred GeV. Details of our analysis, which essentially follows Ref. [62], are given in Appendix B. With the specifications in Eq. (20) it turns out that the dominant operators are the EDM and CEDM of the d quark, generated by two-loop Barr-Zee diagrams [86] as shown in Fig. 2(a,b), and the Weinberg operator which is generated by diagrams Fig. 2(c) with the exchange of a charged Higgs boson. The resulting (C)EDM of the d quark and the gluon CEDM d_W are given in Eqs. (83), (84), and (89), respectively. These three dipole moments depend, apart from the unknown Higgs boson masses M and M_+, on the common unknown factor $\mathrm{Im}\,(\varsigma_u^*\varsigma_d)$ that signifies non-KM *CP* violation. Using the renormalization-group equation for these dipole interactions [24–28] we obtain the following $\not{P}\not{T}$ effective Lagrangian at the scale $\mu = \Lambda_\chi$:

$$\mathcal{L}_{\not{P}\not{T}} = -\frac{d_d(\Lambda_\chi)}{2}\bar{d}i\sigma^{\mu\nu}\gamma_5 d\, F_{\mu\nu} - \frac{\tilde{d}_d(\Lambda_\chi)}{2}\bar{d}i\sigma^{\mu\nu}\gamma_5 t_a d\, G^a_{\mu\nu} + \frac{d_W(\Lambda_\chi)}{6} f_{abc}\varepsilon^{\mu\nu\alpha\beta} G^a_{\alpha\beta} G^b_{\mu\rho} G^{c\,\rho}_{\nu} \ . \tag{21}$$

In order to present the sizes of these dipole moments, we define dimensionless quantities δ_d, $\tilde{\delta}_d$,

[3]The recent papers [82, 85] analyze EDMs in a 2HDM with a Z_2 symmetry and a Higgs potential that softly breaks this symmetry and violates *CP*. They take into account the possibility that the 126 GeV resonance has a (small) *CP*-odd component.

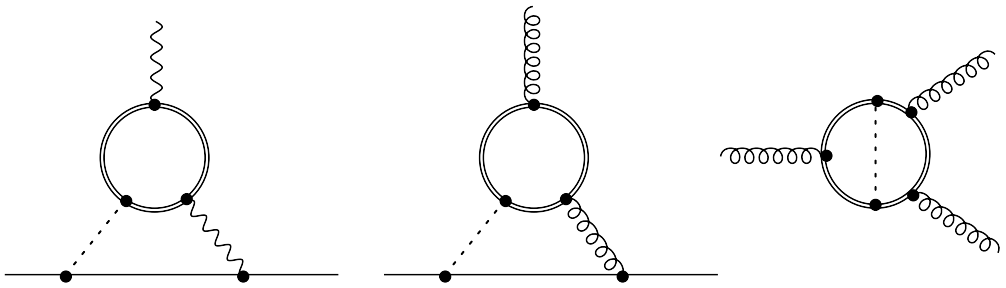

Figure 2: Examples of two-loop diagrams which contribute to the coefficients of the operators in Eq. (21). A single (double) solid lines denotes a light (heavy) quark, a dashed line corresponds to a Higgs boson, and a wavy and a curly line depicts a photon and a gluon, respectively. Diagrams (a,b) are Barr-Zee type diagrams contributing to the quark electric and chromo-electric dipole moment, while diagram (c) contributes to the Weinberg operator.

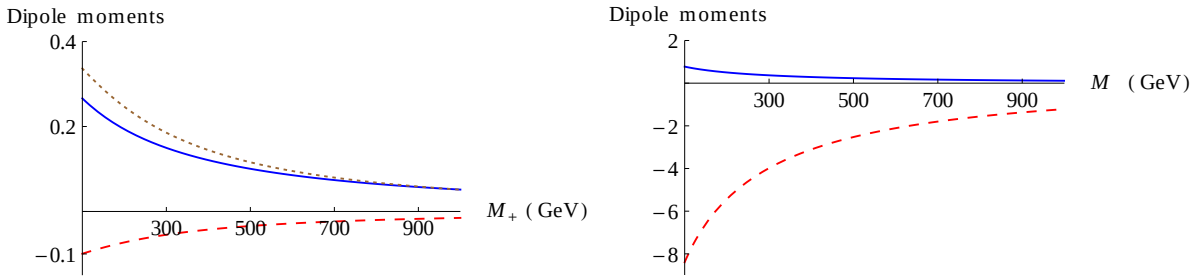

Figure 3: The dimensionless dipole moments δ_d, $\tilde{\delta}_d$, and δ_W, defined in Eq. (22), at the scale Λ_χ as functions of the charged Higgs-boson mass M_+ (left plot) and of the mass M of the neutral Higgs bosons H and A. The blue (solid) and red (dashed) lines correspond to δ_d and $\tilde{\delta}_d$ (we take $g_s > 0$), respectively, and the brown (dotted) line corresponds to δ_W. For the parameter specifications in Eq. (20) there is no contribution to δ_W from the neutral Higgs bosons.

and δ_W by

$$d_d(\Lambda_\chi) = e\delta_d \frac{\bar{m}\,\mathrm{Im}\,(\varsigma_u^*\varsigma_d)}{v^2}\cdot 10^{-4}\,, \quad \tilde{d}_d(\Lambda_\chi) = \tilde{\delta}_d \frac{\bar{m}\,\mathrm{Im}\,(\varsigma_u^*\varsigma_d)}{v^2}\cdot 10^{-4}\,, \quad d_W(\Lambda_\chi) = \delta_W \frac{\mathrm{Im}\,(\varsigma_u^*\varsigma_d)}{v^2}\cdot 10^{-4}\,, \tag{22}$$

where $\bar{m}(\Lambda_\chi) = 4.8$ MeV [63]. The dimensionless moments are given as functions of the mass M_+ of $H^\pm$ and of the mass M of the neutral Higgs bosons H and A in Fig. 3.

The plots in Fig. 3 show that the parameter specifications in Eq. (20) imply that the dominant contribution to the d-quark EDM and to the gluon CEDM d_W is due to charged Higgs boson exchange. In contrast, the contribution of $H^\pm$ to the d-quark CEDM is induced through renormalization-group running and is very small as compared to the contribution of the Higgs bosons H and A to $\tilde{d}_d$. The neutral Higgs bosons also contribute to the d-quark EDM but not to d_W, however, the largest part of $d_d(\Lambda_\chi)$ arises when the d-quark CEDM is renormalization-group evolved to lower energies.

For approximately equal masses of H, A, and the charged Higgs bosons, $M{=}M_H{\simeq}M_A{\simeq}M_+$, we find (numerically) the following Higgs-mass independent relations between the dipole mo-

ments:

$$\tilde{d}_d(\Lambda_\chi) \simeq -7 d_d(\Lambda_\chi)/e \simeq -20 \bar{m} d_W(\Lambda_\chi) \ . \tag{23}$$

Of course, these relations apply only to a very small region in the parameter space of the model. Different hierarchies could be realized. For example, if the charged Higgs boson is significantly lighter than the neutral ones, the dominance of the d-quark CEDM is reduced. However, since there is no good reason to assume $M_+ \ll M_H \approx M_A$, we will use Eq. (23) in what follows. Other hierarchies can be studied in similar fashion. Finally, we recall that in non-supersymmetric 2HDMs with the symmetry breaking scale set by the electroweak scale v, the masses of the Higgs bosons cannot exceed ~ 1 TeV.

2.4 The MSSM

The minimal supersymmetric extension (MSSM) of the Standard Model is another popular SM extension that is theoretically well motivated and allows for non-KM *CP* violation. In general, the soft supersymmetry (SUSY) breaking terms contain many *CP*-violating phases. Often the analysis of *CP*-violating effects is restricted to versions of the MSSM that contain, apart from the KM phase, two additional reparametrization invariant phases, which are usually chosen to be the phase of the μ term and a common phase of the trilinear fermion-sfermion-gaugino interactions. Other SUSY *CP* scenarios are also discussed. For a review, see Ref. [87].

It has been known for a long time [88–91] that SUSY *CP* phases generate EDMs of quarks and charged leptons and CEDMs of quarks at one loop by the exchange of charginos, neutralinos, and gluinos between sfermions and fermions. The Weinberg operator is induced at two loops by diagrams involving gluinos, squarks, and quarks [92]. Moreover, loop-induced SUSY threshold corrections [93] and, in addition, sizable mixing between the two *CP*-even and the *CP*-odd neutral Higgs bosons at one loop [94], which can occur for a certain set of values in the SUSY parameter space, lead to *CP*-violating effects due to neutral Higgs boson exchange. The latter effect induces two-loop (nominally three-loop) Barr-Zee type contributions to the EDMs of quarks and leptons and to the CEDMs of quarks [95–98] and additional two-loop contributions to the Weinberg operator. Two-loop rainbow-like contributions to the (C)EDM of quarks were analyzed in [99, 100]. There is a huge literature on SUSY-induced (C)EDMs that includes Refs. [26, 93, 101–117].

Because the SUSY-induced (C)EDMs of quarks and leptons are quite large, the SUSY particles must be heavy and/or the SUSY phases have to be small in order that the model does not get in conflict with the existing experimental bounds on various EDMs (see below), or cancellations between the various contributions to an atomic/electron EDM and to the EDM of the neutron must occur [102–104, 113]. Another possibility is that flavour-blind SUSY phases are absent and *CP* violation is associated with the SUSY Yukawa interactions, which leads to small EDMs not in conflict with experimental bounds (*cf.*, e.g., Ref. [105]).

Non-observation of SUSY signatures at the LHC so far leads to the conclusion that most of the SUSY particles must be quite heavy if they exist. The interpretation of the LHC data depends of course on the specific SUSY scenario that is used for the data analysis. For instance, the recent global fit [118,119] indicates that the masses of the first and second generation squarks and of the gluinos are above ~ 2 TeV, while the masses of the charginos, neutralinos, and third generation squarks are $\gtrsim 500$ GeV. The lightest of the neutral Higgs bosons is to be identified with the 126 GeV resonance, while the two heavier states H and A and the charged Higgs boson

are above 1 TeV. In scenarios that are in accord with these fit results and assume that the SUSY breaking scale is significantly higher than the electroweak scale, the SUSY phases are nevertheless constrained by the experimental EDM bounds [117].

A comprehensive compilation and analysis of SUSY-induced EDMs of the neutron, deuteron, the Thallium (Tl) and Mercury (Hg) atoms was made in Ref. [114]. (A similar analysis, taking into account more independent SUSY *CP* phases, was performed in Ref. [115].) From this analysis follows that several SUSY *CP* scenarios [98,120,121] induce, for valence u and d quarks, the following $\not{P}\not{T}$ low-energy effective quark-gluon and photon Lagrangian at the scale $\mu = \Lambda_\chi$:

$$\mathcal{L}_{\not{P}\not{T}} = -\frac{1}{2}\sum_{q=u,d}\left(d_q(\Lambda_\chi)\bar{q}i\sigma^{\mu\nu}\gamma_5 q\, F_{\mu\nu} + \tilde{d}_q(\Lambda_\chi)\bar{q}i\sigma^{\mu\nu}\gamma_5 t_a q\, G^a_{\mu\nu}\right) + \frac{d_W(\Lambda_\chi)}{6} f_{abc}\varepsilon^{\mu\nu\alpha\beta}G^a_{\alpha\beta}G^b_{\mu\rho}G^{c\,\rho}_{\nu}\,. \tag{24}$$

In addition, *CP*-violating four-quark operators generated by loop-induced Higgs-boson mediated *CP* violation can be generated. Such operators can also be induced by one-loop box diagrams involving SUSY particles [107], but these are subdominant effects.

The magnitudes and signs of the (C)EDMs of the u and d quarks and of the gluon CEDM in Eq. (24) depend on the masses of the SUSY particles, the sfermion-fermion-gaugino mixing matrix elements, and on the SUSY *CP* phases. For certain sets of SUSY scenarios that are phenomenologically viable, the low-energy effective Lagrangian can be further specified. These scenarios include

a) Heavy SUSY spectrum with a common mass scale > 1 TeV and rather large $\tan\beta = v_2/v_1$. The global fit [119] is in accord with $5 \lesssim \tan\beta \lesssim 30$. In this case the one-loop contributions to the d-quark (C)EDM dominate in Eq. (24), *cf.*, for instance, Ref. [109]. As to *CP*-violating four-quark operators: In view of $\tan\beta \lesssim 30$, of the negative experimental results on SUSY signatures, and of the presently known properties of the 126 GeV resonance (see Sect. 2.3) we conclude that the coefficients of such operators are rather small.

b) Heavy first and second generation sfermions, $m_{\tilde{f}} > 10$ TeV. In this case the contributions to the quark and electron (C)EDMs are suppressed [101] and the dominant contribution to Eq. (24) is due to the Weinberg operator [109].

c) 'Split SUSY' [108]. Here also the third sfermion generation is very heavy, so that sfermions and gluinos decouple from physics at the electroweak scale. In this case the one- and two-loop quark CEDMs and the coefficient of the Weinberg operator are tiny; i.e., the low-energy effective Lagrangian in Eq. (24) contains only the EDMs of the u and d quark that are generated, like the EDM of the electron, by two-loop Barr-Zee type diagrams that involve charginos and neutralinos [108, 111]. In this scenario there is a strong correlation between the magnitudes of the electron and neutron EDM [111].

In summary, several scenarios are possible within the MSSM. However, it appears most natural to us to consider in our analysis of the following sections all $\not{P}\not{T}$ operators of Eq. (24) – which is then similar to the a2HDM. Therefore, in the discussions below we discuss the a2HDM in more detail and only briefly remark at the end of the corresponding sections on the MSSM.

3 The chiral Lagrangian

Below the energy scale $\Lambda_\chi \sim 1$ GeV nonperturbative techniques are required to describe hadronic interactions. The degrees of freedom of the effective field theory of QCD for the two[4] valence quark flavors, $SU(2)$ *Chiral Perturbation Theory* (χPT), are pions (π), nucleons (N) and photons (A_μ) (see, e.g., Ref. [31–35]). The pions are the Goldstone bosons associated with the spontaneous chiral symmetry breakdown $SU(2)_L \times SU(2)_R \to SU(2)_V$. The chiral $SU(2)_L \times SU(2)_R$ symmetry is only approximate and is explicitly broken by the finite quark masses, the quark charges and, in our case, the effective $\not{P}\not{T}$ operators.

The χPT Lagrangian contains all interactions between these fields which are allowed by the symmetries of QCD. Chiral-invariant interactions involving pions always appear with a derivative acting on the pion field and it is this property which gives χPT its consistent power counting. Interactions involving the pion field without derivatives are induced by the chiral-symmetry-breaking interactions in the QCD Lagrangian and are proportional to the small chiral-breaking parameters. This explains the relative lightness of the pion whose mass is proportional to the small average quark mass $m_\pi^2 \sim \bar{m}$.

We are interested in the effects of the $\not{P}\not{T}$ operators appearing in the various scenarios discussed in Sect. 2. They all induce $\not{P}\not{T}$ hadronic interactions, but the form of these interactions differs for each scenario because the various $\not{P}\not{T}$ operators transform differently under chiral and isospin rotations. Each interaction is accompanied by a low-energy constant (LEC) determined by nonperturbative physics. In most cases considered here, these LECs are unknown and, barring lattice QCD calculations, need to be estimated by a model calculation. Reasonable estimates can be obtained by QCD sum rules [11] or naive dimensional analysis (NDA) [29,122]. In the case of the $\bar{\theta}$ term the LECs can be controlled quantitatively, as we will discuss.

The hadronic Lagrangians for the dimension-four and -six operators have been constructed in Refs. [39, 40]. In the next sections we discuss which hadronic operators are induced by the low-energy effective Lagrangians Eqs. (3), (11), (21), and (24). Among the most important of these hadronic operators are the $\not{P}\not{T}$ pion-nucleon interactions, which provide long-range $\not{P}\not{T}$ forces between nucleons. We discuss the $\not{P}\not{T}$ pion-nucleon vertices first. Afterwards we will study the EDMs of the neutron and proton which are not only interesting by themselves but also are an important ingredient of light-nuclear EDMs, to be discussed in subsequent sections.

3.1 Parity- and time-reversal-odd pion-nucleon interactions

Interactions between pions and nucleons that break P and T play an important role in the calculation of the EDMs of nucleons and nuclei because they induce long-range $\not{P}\not{T}$ forces. Historically, hadronic EDMs have often been discussed in terms of a one-boson-exchange model in which it is assumed that P and T violation is induced by the following two[5] nonderivative interactions:

$$\mathcal{L} = \bar{g}_0 \bar{N} \boldsymbol{\pi} \cdot \boldsymbol{\tau} N + \bar{g}_1 \bar{N} \pi_3 N \ . \tag{25}$$

[4] In this work we do not consider the strange quark explicitly which can be done by using $SU(3)$ chiral perturbation theory. We do not expect that effects of dynamical strange quarks exceed the uncertainties given below.

[5] In phenomenological studies a third interaction $\bar{g}_2 \bar{N} \pi_3 \tau_3 N$ is often included as well, but this interaction only appears at higher orders than those considered here for all dimension-four and -six $\not{P}\not{T}$ operators [39, 40].

We discuss below for each scenario the (relative) sizes of the $\bar{g}_i$ and whether additional interactions should be taken into account.

3.1.1 The $\bar{\theta}$ scenario

The $\bar{\theta}$-term is the isospin-conserving element of the same chiral-symmetry breaking quark-antiquark multiplet as the isospin-breaking component of the quark mass matrix – both terms are connected by an axial $SU(2)$ rotation. Therefore, all terms in the effective Lagrangian induced by the $\bar{\theta}$-term are linked to terms arising from the so-called *strong* isospin breaking, i.e., isospin-breaking resulting from the strong interactions [7, 39]. The induced leading-order term in the pion-nucleon sector of the effective Lagrangian is proportional to the quark-mass induced part of the proton-neutron mass difference $(m_n - m_p)^{\text{strong}}$ [123]. It gives the leading contribution to the coupling constant $\bar{g}_0^\theta$ [39, 51, 53],

$$\bar{g}_0^\theta = \frac{(m_n - m_p)^{\text{strong}}(1-\varepsilon^2)}{4F_\pi \varepsilon}\bar{\theta} = (-0.018 \pm 0.007)\,\bar{\theta}\ , \tag{26}$$

where $(m_n - m_p)^{\text{strong}} = (2.6 \pm 0.85)$ MeV [124,125], $\varepsilon \equiv (m_u - m_d)/(m_u + m_d) = -0.35 \pm 0.10$ [63], and $F_\pi = 92.2$ MeV have been used.

The contributions to the coupling constant $\bar{g}_1^\theta$ induced by the $\bar{\theta}$-term can be traced back to the emergence of pion-tadpole terms in the pion-sector Lagrangian, which have to be removed by field redefinitions [39, 51]. These field redefinitions generate the leading contribution to $\bar{g}_1^\theta$ given by [39, 51, 53]:

$$\bar{g}_1^\theta = \frac{2c_1(\delta m_\pi^2)^{\text{strong}}(1-\varepsilon^2)}{F_\pi \varepsilon}\bar{\theta} = (0.003 \pm 0.002)\bar{\theta}\ , \tag{27}$$

where the LEC $c_1 = (-1.0 \pm 0.3)\,\text{GeV}^{-1}$ [126] is related to the nucleon σ-term and where $(\delta m_\pi^2)^{\text{strong}} \simeq (\varepsilon m_\pi^2)^2/(4(m_K^2 - m_\pi^2))$ [127] is the strong contribution to the square of the mass splitting between charged and neutral pions. The uncertainty in Eq. (27) has been increased to account for the contribution to $\bar{g}_1^\theta$ by another independent term [39] in the next-to-next-to-leading-order pion-nucleon Lagrangian [128] with an LEC of unknown strength, which here has been conservatively bounded by its NDA estimate. In fact, a calculation based on resonance saturation predicts only one third of this estimate as an upper bound [51].

In summary, the coupling constant $\bar{g}_1^\theta$ is suppressed with respect to the coupling constant $\bar{g}_0^\theta$ by the ratio $\bar{g}_1^\theta/\bar{g}_0^\theta = -0.2 \pm 0.1$ [51]. This suppression, however, is less than the NDA prediction $|\bar{g}_1^\theta/\bar{g}_0^\theta| = \mathcal{O}(\varepsilon m_\pi^2/\Lambda_\chi^2) \simeq 0.01$ [39].

3.1.2 The minimal left-right symmetric scenario

As discussed in Sect. 2.2, in the mLRSM the most important $\not{P}\not{T}$ contributions at low energies are due to the four-quark interactions in Eq. (11). The chiral Lagrangian induced by these operators has been constructed in Ref. [40] and we recall the main results here. First of all, the two four-quark interactions have the same chiral properties and induce hadronic interactions of identical form (although the LECs, of course, will be different). We therefore use $\text{Im}\,\Xi$ to collectively denote $\eta_{1,8}\,\text{Im}\big(V_L^{ud\,*}\,\Xi_1\big)$ and denote the associated four-quark operator as the four-quark left-right operator (FQLR).

The FQLR is a chiral- and isospin-breaking interaction, however it does not transform under chiral symmetry as any term in the conventional QCD Lagrangian, but instead transforms in a more complicated fashion [40]. The $\not{P}\not{T}$ LECs induced by the FQLR are therefore not linked to any strong LECs as was the case for the $\bar{\theta}$ term. Unfortunately, this implies that we need to resort to different techniques to estimate the LECs. We will use NDA because other methods, such as QCD sum rule estimates are, to our knowledge, not available. Nevertheless, even without detailed knowledge of the LECs, considerations based on chiral symmetry give a lot of information on the hierarchy of the hadronic interactions.

Because the FQLR violates isospin symmetry it does not contribute to $\bar{g}_0^{\rm LR}$ directly. Instead, it contributes to isospin-violating LECs in two ways. First of all, a pion tadpole is induced. However, due to the complicated chiral properties of the FQLR, this tadpole is associated with a three-pion vertex [40] which, in the so-called σ-parametrization of $SU(2)$ χPT, see e.g., Ref. [129], reads

$$\mathcal{L}^{\rm LR} = \bar{\Delta}^{\rm LR} F_\pi \pi_3 \left(1 - \frac{\boldsymbol{\pi}^2}{2F_\pi^2}\right) \ . \tag{28}$$

In addition, the FQLR induces a direct contribution to $\bar{g}_1^{LR}$. The sizes of the LECs can be estimated by NDA:

$$|\bar{\Delta}^{\rm LR}| = \mathcal{O}(F_\pi^2 \Lambda_\chi^2 {\rm Im}\,\Xi) \simeq (0.01\,{\rm GeV}^4){\rm Im}\,\Xi \ , \ \ |\bar{g}_1^{\rm LR}| = \mathcal{O}(F_\pi \Lambda_\chi {\rm Im}\,\Xi) \simeq (0.1\,{\rm GeV}^2){\rm Im}\,\Xi \, . \tag{29}$$

Just as for the $\bar{\theta}$ term, the tadpole can be removed using field redefinitions. However, differently from the $\bar{\theta}$ term, a three-pion vertex is left behind (see Eq. (32)). Moreover, the removal of the tadpole induces an additional contribution to $\bar{g}_1^{\rm LR}$ proportional to $\bar{\Delta}^{\rm LR}$:

$$\bar{g}_1^{\rm LR} \to \bar{g}_1^{\rm LR} + \bar{g}_1^{\rm LR\prime} \ , \qquad \bar{g}_1^{\rm LR\prime} = -\frac{4c_1 \bar{\Delta}^{\rm LR}}{F_\pi} \ . \tag{30}$$

Since $c_1 = \mathcal{O}(1/\Lambda_\chi)$, the additional contribution is formally of the same order as the original term. However, numerically it might be somewhat larger because $4c_1$ is bigger than expected from NDA. In addition, a first non-vanishing contribution to $\bar{g}_0^{\rm LR\prime}$ appears[6], also proportional to $\bar{\Delta}^{\rm LR}$:

$$\bar{g}_0^{\rm LR\prime} = -\frac{(m_n - m_p)^{\rm strong} \bar{\Delta}^{\rm LR}}{2m_\pi^2 F_\pi} \ . \tag{31}$$

In conclusion, the relevant pionic and pion-nucleon interactions are given by

$$\mathcal{L}^{\rm LR} = -\bar{\Delta}^{\rm LR} \frac{\pi_3 \boldsymbol{\pi}^2}{2F_\pi} + \bar{g}_0^{\rm LR\prime} \bar{N} \boldsymbol{\pi} \cdot \boldsymbol{\tau} N + (\bar{g}_1^{\rm LR} + \bar{g}_1^{\rm LR\prime}) \bar{N} \pi_3 N \ . \tag{32}$$

Because $\bar{g}_0^{\rm LR\prime}$ and $\bar{g}_1^{\rm LR\prime}$ both depend on the same LEC $\bar{\Delta}^{\rm LR}$, their ratio depends only on known quantities:

$$\frac{\bar{g}_0^{\rm LR\prime}}{\bar{g}_1^{\rm LR\prime}} = \frac{(m_n - m_p)^{\rm strong}}{8c_1 m_\pi^2} = -0.02 \pm 0.01 \ . \tag{33}$$

Unless $\bar{g}_1^{\rm LR}$ and $\bar{g}_1^{\rm LR\prime}$ cancel to a high degree – which is not expected on any grounds – the coefficient $\bar{g}_0^{\rm LR\prime}$ is much smaller [40] than the combination $\bar{g}_1^{\rm LR} + \bar{g}_1^{\rm LR\prime}$ which appears in observables. From now on, we relabel $\bar{g}_1^{\rm LR} + \bar{g}_1^{\rm LR\prime} \to \bar{g}_1^{\rm LR}$ and $\bar{g}_0^{\rm LR\prime} \to \bar{g}_0^{\rm LR}$, and take $|\bar{g}_0^{\rm LR}/\bar{g}_1^{\rm LR}| \ll 1$. This result is in stark contrast with the $\bar{\theta}$ scenario where $\bar{g}_0^{\bar{\theta}}$ is the dominant interaction. This difference has important consequences for light-nuclear EDMs.

[6] If the $\bar{\theta}$ term is removed by the Peccei-Quinn mechanism, this contribution to $\bar{g}_0^{\rm LR\prime}$ would be absent [130]. Because it is small anyway this has no consequences for our analysis.

3.1.3 The a2HDM and MSSM scenarios

Next we discuss the hierarchy of pion-nucleon interactions which emerges in the scenario of Sects. 2.3 and 2.4. In the a2HDM and MSSM scenarios we must compare the contributions from the three operators appearing in Eqs. (21) and (24). We focus first on the a2HDM scenario because here we have some idea on the relative sizes of the quark (C)EDMs and the Weinberg operator. After discussing the a2HDM, we consider briefly how our findings might be altered in the MSSM.

The contributions from the qEDM to the pion-nucleon LECs are highly suppressed because of the appearance of the photon which needs to be integrated out. As such, the qEDM contributions are suppressed by the typical factor $\alpha_{\rm em}/\pi \sim 10^{-3}$ and can be safely neglected. Because the Weinberg operator conserves chiral symmetry, it cannot directly induce the $\not{P}\not{T}$ pion-nucleon couplings which break chiral symmetry [131]. Instead, an additional insertion of the quark mass (difference) is required which implies, by NDA, that the LECs scale as $|\bar{g}_0^{\rm H}| = \mathcal{O}(\bar{m}\Lambda_\chi\, d_W)$ and $|\bar{g}_1^{\rm H}| = \mathcal{O}(\varepsilon\bar{m}\Lambda_\chi\, d_W)|$ [46]. On the other hand, the down quark CEDM in Eq. (21) can induce the pion-nucleon couplings directly such that, for this source, $|\bar{g}_{0,1}^{\rm H}| = \mathcal{O}(\Lambda_\chi\, \tilde{d}_d)$ [46]. Together with the observation that $\bar{m}|d_W|$ is about an order of magnitude smaller than $|\tilde{d}_d|$ in the model under investigation, we conclude that the pion-nucleon couplings are dominated by the qCEDM.

To check whether the NDA estimate is reasonable we compare it to results obtained in Refs. [11, 132] where the pion-nucleon LECs were investigated in the framework of QCD sum rules. It was found that[7]

$$\bar{g}_1^{\rm H} = -(2^{+4}_{-1}\,\text{GeV})\,\tilde{d}_d\ , \qquad \bar{g}_0^{\rm H} \simeq (0.5 \pm 1)\,\text{GeV}\,\tilde{d}_d\ . \tag{34}$$

The coupling $\bar{g}_1^{\rm H}$ is somewhat bigger than the NDA estimate but not in disagreement. The calculation of $\bar{g}_0^{\rm H}$ has a relatively larger uncertainty (even an uncertain sign) which is also harder to quantify [132]. The size of $\bar{g}_0^{\rm H}$ is somewhat smaller than $\bar{g}_1^{\rm H}$, and it is in agreement with NDA.

Considering the large uncertainties in these estimates, from now on we will take for the a2HDM scenario that $|\bar{g}_0^{\rm H}| \simeq |\bar{g}_1^{\rm H}|$ as indicated by NDA. However, there is a significant uncertainty involved and the only way to improve the situation is, most likely, a direct lattice calculation.

The situation in the MSSM is similar. Unless the Weinberg operator is larger than the u and d quark CEDMs, also in this scenario the pion-nucleon LECs are dominated by the qCEDM contributions. The u-quark CEDM is now expected to be significant as well which means that the result in Eq. (34) should be slightly altered: $\tilde{d}_d$ in the expression for $\bar{g}_1$ ($\bar{g}_0$) should be replaced by $\tilde{d}_d - \tilde{d}_u$ ($\tilde{d}_d + \tilde{d}_u$). Nevertheless, we expect again that the pion-nucleon LECs are of similar size, with the possibility that $|\bar{g}_1^{\rm MSSM}|$ is slightly larger than $|\bar{g}_0^{\rm MSSM}|$. Even in the case that the Weinberg operator is much larger than the quark CEDMs, a large hierarchy between $\bar{g}_0^{\rm MSSM}$ and $\bar{g}_1^{\rm MSSM}$ is not expected to appear. The NDA estimates given above tell us that the LECs are of similar size, apart from a possible small suppression of $\bar{g}_1^{\rm MSSM}$ due to insertion of the quark-mass difference ε. In what follows we therefore take $|\bar{g}_0^{\rm MSSM}| \simeq |\bar{g}_1^{\rm MSSM}|$.

[7] It should be noted that these results assume a Peccei-Quinn mechanism to remove the $\bar{\theta}$ term. This also shifts the qCEDM contributions to pion-nucleon LECs. However, the order of magnitude stays the same. Since we use these results as a sanity check of the NDA estimate, this poses no real problem.

3.2 The EDMs of the neutron and proton

Now that we have discussed the $\not{P}\not{T}$ pion-nucleon interactions for each of the scenarios we turn to the calculation of the nucleon EDMs. The nucleon EDMs obtain contributions from one-loop diagrams involving the $\not{P}\not{T}$ pion-nucleon vertices in Eq. (25). However, these diagrams are ultraviolet-divergent and renormalization requires counterterms to absorb these divergences and the associated scale dependence. Such counterterms appear naturally in χPT in the form of $\not{P}\not{T}$ nucleon-photon vertices [41–48],

$$\mathcal{L}_{N\gamma} = -2\,\bar{N}\left(\bar{d}_0 + \bar{d}_1\tau_3\right) S^\mu N\, v^\nu F_{\mu\nu} \ , \tag{35}$$

in terms of the nucleon spin $S^\mu = (0\,,\,\vec{\sigma}/2)^T$ and velocity $v^\mu = (1\,,\,\vec{0})^T$ in the nucleon rest-frame. These counterterms appear in all scenarios discussed here, but their sizes, of course, vary depending on the scenario under investigation.

Before discussing the new LECs $\bar{d}_{0,1}$, let us first discuss the calculation of the nucleon EDM in terms of $\not{P}\not{T}$ interactions in Eqs. (25) and (35)[8]. This calculation has been performed in $SU(2)_L \times SU(2)_R$ heavy-baryon χPT up to next-to-leading order in Refs. [43, 46, 47] (for $SU(3)_L \times SU(3)_R$ results, see Refs. [42,45,48]) and gives for the neutron (d_n) and proton EDM (d_p)

$$\begin{aligned} d_n &= \bar{d}_0 - \bar{d}_1 - \frac{e g_A \bar{g}_0}{8\pi^2 F_\pi}\left(\ln\frac{m_\pi^2}{m_N^2} - \frac{\pi m_\pi}{2m_N}\right) \ , \\ d_p &= \bar{d}_0 + \bar{d}_1 + \frac{e g_A}{8\pi^2 F_\pi}\left[\bar{g}_0\left(\ln\frac{m_\pi^2}{m_N^2} - \frac{2\pi m_\pi}{m_N}\right) - \bar{g}_1\frac{\pi m_\pi}{2m_N}\right] \ , \end{aligned} \tag{36}$$

where $e > 0$. Furthermore, $g_A \simeq 1.27$ is the strong pion-nucleon coupling constant [63], m_N the nucleon mass, and the divergence has been absorbed into the counterterms. The leading loop result reproduces the famous result obtained in Ref. [7], where current algebra techniques were applied.

The dependence of the nucleon EDMs on the LECs $\bar{d}_{0,1}$ implies that considerations based on chiral symmetry alone cannot tell us the sizes of these EDMs. Even in the $\bar{\theta}$ scenario, in which we have relatively precise knowledge of the LECs $\bar{g}_{0,1}$ (see Eqs. (26) and (27)), the exact dependence of d_n and d_p on $\bar{\theta}$ is unclear due to the unknown finite parts of $\bar{d}_{0,1}$. The same holds, of course, for the other scenarios, where not even the LECs $\bar{g}_{0,1}$ are known precisely. Thus, the EDM results in the nucleon case alone are of limited use to get information on the physics that generated them. The strength of our methods will become much more visible when two-nucleon contributions, i.e., the cases of the deuteron and tri-nucleon EDMs, will be investigated in Sect. 4. To get quantitative information on the nucleon EDMs other techniques are necessary. Let us now, for each of the scenarios, discuss the sizes of the nucleon EDMs.

3.2.1 The $\bar{\theta}$ scenario

By inserting the values of $\bar{g}_{0,1}$ from Eqs. (26) and (27) into Eq. (36) it is possible to evaluate the loop contributions to the nucleon EDMs:

$$d_n^{\bar{\theta},\mathrm{loop}} = (-2.5 \pm 0.9)\cdot 10^{-16}\,\bar{\theta}\,e\,\mathrm{cm} \ , \qquad d_p^{\bar{\theta},\mathrm{loop}} = (2.8 \pm 0.9)\cdot 10^{-16}\,\bar{\theta}\,e\,\mathrm{cm} \ . \tag{37}$$

[8] Contributions from the three-pion vertex $\bar{\Delta}^{\mathrm{LR}}$ in Eq. (32) to the nucleon EDM vanish up to next-to-leading order [40].

This sets the scale for the nucleon EDM but the actual numbers can change due to the LECs $\bar{d}_{0,1}$. The sizes of the LECs can be estimated by NDA. This yields

$$|\bar{d}^{\bar{\theta}}_{0,1}| = \mathcal{O}\left(e\bar{\theta}\,\frac{m_\pi^2}{\Lambda_\chi^3}\right) \simeq 3\cdot 10^{-16}\,\bar{\theta}\,e\,\text{cm}\ , \tag{38}$$

which is of similar size as the loop contributions. By combining a χPT calculation with lattice QCD data, it recently became possible to compute the total nucleon EDM (loop and tree-level contributions) [48]. It was found that[9]

$$d_n^{\bar{\theta}} = (-2.9\pm 0.9)\cdot 10^{-16}\,\bar{\theta}\,e\,\text{cm}\ , \qquad d_p^{\bar{\theta}} = (1.1\pm 1.1)\cdot 10^{-16}\,\bar{\theta}\,e\,\text{cm}\ , \tag{39}$$

which is the result we will use in what follows. For the deuteron EDM, an important quantity is the sum of the nucleon EDMs which is

$$d_n^{\bar{\theta}} + d_p^{\bar{\theta}} = (-1.8\pm 1.4)\cdot 10^{-16}\,\bar{\theta}\,e\,\text{cm}\ , \tag{40}$$

with a significant uncertainty.

3.2.2 The minimal left-right symmetric scenario

In the case of the mLRSM the situation is far more uncertain than for the $\bar{\theta}$ term. Because $\bar{g}_0^{\text{LR}}$ is significantly suppressed (see Eq. (33)), this implies that the loop contributions proportional to $\bar{g}_0^{\text{LR}}$ are actually subleading. Up to next-to-leading order the neutron EDM does not depend on $\bar{g}_1^{\text{LR}}$, and therefore in Ref. [74] the calculation was extended to next-to-next-to-leading order. It was concluded that both the neutron and proton EDM obtain dominant contributions from the LECs $\bar{d}_{0,1}$, while the loop contributions are an order of magnitude smaller. Unfortunately, the exact sizes of the EDMs as function of the fundamental mLRSM parameter $\text{Im}\,\Xi$ is rather uncertain. There exists, to our knowledge, no reliable model calculation. Therefore we cannot do better than NDA, which gives

$$|d_{n,p}| = \mathcal{O}\left(e\text{Im}\,\Xi\frac{F_\pi^2}{\Lambda_\chi}\right) \simeq (10\,\text{MeV})\,e\text{Im}\,\Xi\ , \tag{41}$$

with an unknown sign and a large uncertainty in its magnitude.

3.2.3 The a2HDM and MSSM scenarios

Both within the a2HDM and the MSSM, the nucleon EDMs obtain contributions from each of the three operators in Eqs. (21) and (24), respectively. For the pion-nucleon interactions we were fortunate that one of the operators gave dominant contributions which simplified the analysis. For the nucleon EDM we do not have this advantage because the qEDM and Weinberg operator induce the tree-level LECs $\bar{d}_{0,1}$ without additional suppressions [46]. As a consequence, we need to study all three operators.

To be specific we start the discussion with the a2HDM. The discussion in Sect. 3.1.3 tells us that the loop contributions to the nucleon EDMs are dominated by the qCEDM because the

[9] Lattice data at lower pion masses, where the chiral extrapolations will be more reliable, are expected to become available soon. A new look at the single-nucleon EDM predictions is work in progress.

$\not{P}\not{T}$ pion-nucleon LECs are suppressed for the qEDM and Weinberg operator. Using the NDA estimate for $\bar{g}_0$ (in good agreement with the QCD sum rules result [132]) gives

$$|d_n^{\mathrm{H,\,loop}}| \simeq -|d_p^{\mathrm{H,\,loop}}| \simeq (0.7)\, e\tilde{d}_d \ , \tag{42}$$

in terms of the down-quark CEDM $\tilde{d}_d$. The tree-level terms $\bar{d}_{0,1}$ obtain contributions from all operators. NDA tells us [46]:

$$\left|d_{n,p}^{\mathrm{H,\,tree}}\right| = \mathcal{O}\left(d_d,\ \frac{e\tilde{d}_d}{4\pi},\ F_\pi\, e d_W\right) \simeq \left(d_d,\ (0.1)\, e\tilde{d}_d,\ (0.1\,\mathrm{GeV})\, e\, d_W\right) \ , \tag{43}$$

which implies that the loop contributions of the qCEDM are larger than its tree-level contributions. The approximate hierarchy of the dipole moments $\tilde{d}_d \simeq -7\, d_d/e \simeq -20(\bar{m} d_W)$ (with $\bar{m} \simeq 5$ MeV) obtained in Sect. 2.3, shows that the nucleon EDMs obtain contributions comparable in magnitude from all three operators, with perhaps a slight dominance of the Weinberg operator (although this is questionable, see the discussion below). Of course, these estimates are very rough and can in no way be used to make a definite statement about the exact sizes of the nucleon EDMs in the a2HDM scenario that we investigate. They only provide an approximate scale for the EDMs.

The nucleon EDM induced by the qEDM, qCEDM, and Weinberg operator has been investigated extensively in the literature (see Refs. [11, 12] for reviews). In particular, the calculation for all three operators has been performed with QCD sum rules [11, 53, 131, 133]. The authors of these references obtained, in our notation[10, 11, 12],

$$d_n = (1 \pm 0.5)\left(1.4\, d_d - 0.55\, e\tilde{d}_d\right) \pm (0.02\,\mathrm{GeV})\, e d_W \ , \tag{44}$$

with an unspecified, but significant error (and sign) on the coefficient of the Weinberg operator. The hierarchy between d_d, $\tilde{d}_d$, and d_W then indicates that all operators contribute at the same level to the neutron EDM. The qEDM and qCEDM results are in good agreement with the chiral loop results and NDA. The result for the Weinberg operator is somewhat smaller (see the discussion in Ref. [131]) but, in view of the large uncertainties involved, the estimates are not really in disagreement. The isoscalar combination $d_n + d_p$ has also been estimated with QCD sum rules [53],

$$d_n + d_p = (0.5 \pm 0.3)\, d_d - (0.2 \pm 0.1)\, e\tilde{d}_d \pm (0.02\,\mathrm{GeV})\, e d_W \ , \tag{45}$$

with slightly smaller coefficients in front of the qEDM and qCEDM than in the case of the neutron EDM.

To summarize, in the a2HDM scenario of Sect. 2.3, the nucleon EDMs get contributions of roughly equal size from the d-quark EDM and CEDM and the Weinberg operator. The rather large uncertainties in magnitude and sign of each of these contributions make it impossible to

[10] As before, a Peccei-Quin mechanism was used to remove the $\bar{\theta}$ term.

[11] The difference between our d-quark CEDM $\tilde{d}_d$ and the one found in Refs. [11, 133] is due to an explicit factor of $g_s(\Lambda_\chi) \simeq 2$ that appears in the definition of the qCEDM in these references.

[12] A similar calculation was performed in Ref. [134] which found somewhat smaller coefficients for the qEDM and qCEDM. On the other hand, larger coefficients were found in Ref. [135]. These differences show that the uncertainties are large.

obtain a firm prediction of the sizes of the nucleon EDMs. We conclude that we cannot really do better than give a rough estimate of the combined contributions which sets the scale for the sizes of both the neutron and proton EDM:

$$|d_{n,p}| = \mathcal{O}(e\,\tilde{d}_d) \ , \tag{46}$$

and we do not expect the nucleon EDMs to be larger than this estimate.

When switching to the MSSM, the above relations should include the dependence on the u-quark (C)EDM. In the most general case one may expect comparable contributions from the q(C)EDMs and the Weinberg operator to the nucleon EDMs. The above analysis of the a2HDM would then roughly hold for the MSSM as well. However, the MSSM allows for different hierarchies between the dipole operators as well, *cf.* the discussion at the end of subsection 2.4. For example, in the 'split SUSY' scenario of Ref. [108] the nucleon EDMs would be given directly in terms of the quark EDMs.

3.3 A short intermediate summary

Before we proceed to the discussion of light-nuclear EDMs, let us briefly summarize what we found so far. We have seen that the different scenarios of Sect. 2 predict distinct hierarchies for the $\not{P}\not{T}$ pion-nucleon interactions in Eq. (25). Roughly, we find $\bar{g}_1^{\bar{\theta}}/g_0^{\bar{\theta}} \simeq -0.2$ for the $\bar{\theta}$ term [51], $\bar{g}_1^{\rm LR}/\bar{g}_0^{\rm LR} \simeq -50$ for the mLRSM [40], and $|\bar{g}_0^{\rm H}| \simeq |\bar{g}_1^{\rm H}|$ and $|\bar{g}_0^{\rm MSSM}| \simeq |\bar{g}_1^{\rm MSSM}|$ in the a2HDM and MSSM scenarios (although $|\bar{g}_1^{H}|$ might be somewhat larger than $|\bar{g}_0^{H}|$ [132]).

This information, however, does not lead to a solid prediction of the sizes of the neutron and proton EDM apart from the expectation that, in all scenarios, they are of comparable size. The lack of predictive power is mainly caused by the fact that the nucleon EDMs obtain leading-order contributions from tree-level diagrams independent of the $\not{P}\not{T}$ pion-nucleon interactions. The situation is somewhat better for the $\bar{\theta}$ term (see Ref. [48]) because of lattice data, but the uncertainties, in particular for the proton EDM, are still significant. Lattice efforts are underway to improve this situation. For the higher-dimensional BSM sources little progress is expected in the near future.

A signal in a single EDM measurement would, of course, not point to its origin. The above considerations imply that, at the moment, even a measurement of both the proton and neutron EDM is not enough to disentangle the various scenarios [46] (although a hint for the $\bar{\theta}$ term might be found). Additional measurements are therefore required, and in the next sections we will argue that light-nuclear EDM experiments are excellent probes for this task. In Sect. 5 we discuss EDMs of heavier systems which provide complementary information.

4 EDMs of light nuclei

The power of the χPT approach becomes much more manifest in few-nucleon systems. First of all, the EDMs of light nuclei can be accurately calculated in terms of the $\not{P}\not{T}$ hadronic interactions. The associated nuclear uncertainties are much smaller than the hadronic uncertainties appearing in the LECs themselves. Moreover, while the $\not{P}\not{T}$ pion-nucleon vertices only contribute to the nucleon EDM at the one-loop level, which brings in a loop suppression and counterterms, light-nuclear EDMs depend already at tree-level on the pion-nucleon vertices and counterterms only appear at subleading orders.

In Refs. [50, 51] EFTs[13] have been constructed with which controlled calculations of light-nuclear EDMs can be performed. In fact, this has already been done for the EDMs of the deuteron and tri-nucleon system. The calculations in Refs. [50, 51] used a so-called 'hybrid' approach in which the nuclear wave functions were calculated using modern phenomenological potentials while the $\not{P}\not{T}$ potential and currents were calculated using chiral EFT. Recently, these calculations have been repeated using chiral EFT for both the PT-even and -odd parts of the problem [54, 55]. Although, the results of the hybrid and full EFT calculations are very similar, the latter approach has the advantage that the nuclear uncertainty can be quantified by varying the cut-off parameters that appear in the solution of the scattering equations. This gives us a quantitative handle on the nuclear uncertainties which turn out to be small compared to the hadronic uncertainties in the $\not{P}\not{T}$ LECs themselves.

Before going to the actual results a few comments are in order. Based on chiral symmetry considerations, it was argued in Ref. [50] that light-nuclear EDMs should be calculated in terms of six LECs. So far we have only encountered four, namely the $\not{P}\not{T}$ pion-nucleon LECs $\bar{g}_0$ and $\bar{g}_1$ and the nucleon EDMs d_n and d_p[14]. The other two LECs introduced in Ref. [50] are associated with $\not{P}\not{T}$ nucleon-nucleon contact interactions of the form

$$\mathcal{L}_{NN} = \bar{C}_1 \bar{N} N \, \partial_\mu (\bar{N} S^\mu N) + \bar{C}_2 \bar{N} \boldsymbol{\tau} N \cdot \partial_\mu (\bar{N} S^\mu \boldsymbol{\tau} N) \ . \tag{47}$$

For the $\bar{\theta}$ term and most of the higher-dimensional BSM operators discussed above these contact interactions appear at high order in the chiral Lagrangians and their effects are negligible compared to the one-pion exchange between nucleons proportional to $\bar{g}_{0,1}$ [136]. However, for chiral-invariant sources such as the Weinberg operator, the $\not{P}\not{T}$ pion-nucleon LECs are suppressed and the terms in Eq. (47) appear at the same order as $\bar{g}_{0,1}$. Nevertheless, the terms in Eq. (47) only play a marginal role as we will discuss in more detail below.

The three-pion vertex with LEC $\bar{\Delta}^{\rm LR}$ appearing in Eq. (32) was not considered in Ref. [50]. Although it has little consequences for the nucleon and deuteron EDMs, it introduces a potentially important $\not{P}\not{T}$ three-body interaction [40] which could affect the ^{3}He and ^{3}H EDMs. This has not been taken into account so far.

4.1 The EDM of the deuteron

The EDM of the lightest bound nucleus, the deuteron, has been investigated in a number of papers in recent years [49–51, 53, 55, 137–140]. From a theoretical point of view, the deuteron is particularly interesting. Not only because it is a rather simple nucleus which can be accurately described, but also because its spin-isospin properties ensure that the deuteron EDM has rather distinctive properties.

At leading order in the EFT, the deuteron EDM obtains two contributions. The first one is simply the contribution from the constituent nucleon EDMs which is trivially evaluated as $d_n + d_p$. The second contribution is due to the exchange of a single pion between the nucleons involving a $\not{P}\not{T}$ pion-nucleon vertex (i.e., $\bar{g}_0$ or $\bar{g}_1$) and the coupling of the external photon to the proton charge. All calculations are consistent and here we quote the central value and uncertainty of the chiral EFT result [54, 55]:

$$d_D = d_n + d_p + \big[(0.18 \pm 0.023)\, \bar{g}_1 + (0.0028 \pm 0.0003)\, \bar{g}_0\big] e \,\text{fm} \,, \tag{48}$$

[13] The EFTs differ somewhat in their power counting, but the leading results are identical.

[14] In this section we will treat the EDMs d_n and d_p as effective parameters. The reason is that the part of $d_{n,p}$ depending on $\bar{g}_{0,1}$ cannot be isolated from the tree-level LECs $\bar{d}_{0,1}$ in a model-independent way.

which is almost independent of $\bar{g}_0$. This can be understood from the following reasoning: The deuteron ground state is a ${}^3S_1$ state with a small ${}^3D_1$ admixture. After a pion exchange involving a leading $\bar{g}_0$ vertex which conserves the total isospin, the wave function obtains a small ${}^1P_1$ component. Because the electric interaction with the proton charge is spin-independent, it cannot return the wave function to its ${}^3S_1$-${}^3D_1$ ground state and the contribution vanishes. By exactly the same argument the leading contributions from the NN contact interactions in Eq. (47) vanish for the deuteron [49].

The systematic nature of the EFT approach used in Refs. [50, 51] allows the calculation of higher-order corrections, for example, due to two-pion-exchange diagrams [136] or two-body currents. Such corrections give rise to the small dependence of d_D on $\bar{g}_0$. We now turn to the implications of this result for the various scenarios.

4.1.1 The $\bar{\theta}$ scenario

In this scenario the deuteron EDM can be given as a function of $\bar{\theta}$. It follows from Eqs. (26), (27), (40), and (48) that

$$d_D^{\bar{\theta}} = [(-1.8 \pm 1.4) + (0.55 \pm 0.36 \pm 0.054) - (0.05 \pm 0.02 \pm 0.006)] \cdot 10^{-16}\, \bar{\theta}\, e\,\mathrm{cm} \ , \tag{49}$$

where the first term is the contribution from the nucleon EDMs and the second and third, respectively, from the two-body contribution proportional to $\bar{g}_1^{\bar{\theta}}$ and $\bar{g}_0^{\bar{\theta}}$. The first error of the coefficients is due the hadronic uncertainty in the LECs (see Eqs. (26) and (27)), while the second error of the last two terms is due to the nuclear uncertainty. The hadronic uncertainty is significantly larger than the nuclear uncertainty.

We can learn a few things from Eq. (49). First of all, the deuteron is most likely dominated by the nucleon EDMs, although the uncertainties are still too large to say this with full confidence [50]. More input from lattice calculations is needed to improve the situation. Second, when measurements of d_n, d_p, and d_D will be available, the relation

$$d_D^{\bar{\theta}} - d_n^{\bar{\theta}} - d_p^{\bar{\theta}} = (5.0 \pm 3.7) \cdot 10^{-17}\, \bar{\theta}\, e\,\mathrm{cm} \tag{50}$$

will be a promising and relatively precise method to directly extract the value of $\bar{\theta}$ from experiments [51]. The existence of the $\bar{\theta}$ term can then be tested in several ways. One can compare the experimental value of d_n and/or d_p to lattice calculations. A more robust test, independent of lattice results, would be the measurement of the ^{3}He or ^{3}H EDM whose dependence on $\bar{\theta}$ can be firmly predicted. We will discuss this in Sect. 4.2.1.

4.1.2 The mLRSM scenario

The mLRSM scenario is in general more uncertain than the $\bar{\theta}$ term. Because $\bar{g}_0^{\mathrm{LR}}/\bar{g}_1^{\mathrm{LR}} \ll 1$ (see Eq. (33)) we can safely ignore the $\bar{g}_0$ term in Eq. (48). Inserting the NDA estimates[15] given in Eqs. (29) and (41) into the expression for the deuteron EDM, we obtain

$$\left|d_D^{\mathrm{LR}}\right| = \left|(10\,\mathrm{MeV})\, e\mathrm{Im}\Xi \ \pm\ (100\,\mathrm{MeV})\, e\mathrm{Im}\Xi\right| \ , \tag{51}$$

[15] Note that the size of $\bar{g}_1^{\mathrm{LR}}$ might be somewhat larger than the NDA estimate due to the large size of the term $4c_1$, see the discussion after Eq. (30). The estimate used here is conservative.

where the first term is due to the nucleon EDMs and the second term is the two-body contribution.

These rough estimates tell us that the two-body contribution to the dEDM is about an order of magnitude larger than the sum of the nucleon EDMs. Without detailed information on the LECs (for which input from lattice calculations is required) this statement cannot be made much more precise. Nevertheless, the difference between the ratios of deuteron-to-nucleon-EDMs for the $\bar{\theta}$ and the mLRSM scenario tell us that a deuteron EDM experiment would be complementary to nucleon EDM experiments. In particular, a large deuteron-to-nucleon EDM ratio would be indicative of BSM physics [49, 53], in particular of the mLRSM scenario.

4.1.3 The a2HDM and MSSM scenarios

The situation for the a2HDM is somewhat similar to that of the mLRSM. The $\bar{g}_0^{\mathrm{H}}$ term in Eq. (48) can be neglected since we expect $|\bar{g}_0^{\mathrm{H}}| \simeq |\bar{g}_1^{\mathrm{H}}|$, while the coefficient in front of $\bar{g}_0^{\mathrm{H}}$ is a hundred times smaller. Using the estimates from Sects. 3.1.3 and 3.2.3 gives

$$d_D^{\mathrm{H}} = \pm(e\,\tilde{d}_d) \;-\; (2^{+4}_{-1})e\,\tilde{d}_d \;\;, \tag{52}$$

where the first term is due to the nucleon EDMs[16] and the second term results from the two-body contribution. The uncertainty of the two-body contribution is obtained from the QCD sum rules estimate of $\bar{g}_1^H$ [132]. The nuclear uncertainty is neglected since it is at least an order of magnitude smaller.

In the a2HDM scenario the deuteron-to-nucleon EDM ratio lies between the $\bar{\theta}$ and mLRSM scenarios discussed above. It can be expected that the deuteron EDM is a few times bigger than the sum of the nucleon EDMs. However, it must be stressed that the nucleon EDMs obtain contributions from three different BSM operators, *cf.* Eq. (21). Therefore, the accumulated uncertainty is significant. In particular the uncertainty associated with the Weinberg operator is large. Therefore, the conclusion $|d_D^{\mathrm{H}}| > |d_n^{\mathrm{H}} + d_p^{\mathrm{H}}|$ might be premature.

As discussed in Sect. 3.1.3 also in the MSSM we expect $|\bar{g}_0^{\mathrm{MSSM}}| \simeq |\bar{g}_1^{\mathrm{MSSM}}|$ which means we can again neglect the $\bar{g}_0$ term in Eq. (48). However, in the MSSM it is even harder to make a statement about the size of d_D with respect to $d_{n,p}$. In case the qCEDM is significant we expect similar results as in the a2HDM. On the other hand, if the qEDMs and/or the Weinberg operator are large with respect to the qCEDM, the relation $d_D = d_n + d_p$ should hold to good approximation. More refined statements should become possible, once the parameter space of the MSSM is further constrained.

4.1.4 The deuteron EDM: an overview

Let us briefly summarize the results on the dEDM in the above scenarios. In case of the QCD $\bar{\theta}$ term, the dEDM is a relatively well understood quantity and can be directly expressed as a function of the fundamental parameter $\bar{\theta}$. Results so far indicate that the value of the dEDM is rather close to the sum of the nucleon EDMs, while the relatively small difference $d_D^{\bar{\theta}} - d_n^{\bar{\theta}} - d_p^{\bar{\theta}}$ provides a good method to extract the value of $\bar{\theta}$.

[16] We most likely overestimate the nucleon EDM contribution to d_D^{H} since $d_n^{\mathrm{H}} + d_p^{\mathrm{H}}$ is expected to be smaller than d_n^{H} and d_p^{H} individually, see Eqs. (44) and (45).

The situation is different for the other three scenarios. Both for the mLRSM and the a2HDM we expect

$$\left|\frac{d_D - d_n - d_p}{d_n + d_p}\right| > 1 \ . \tag{53}$$

However, the exact value of this ratio is uncertain. In the mLRSM, NDA suggests that the dEDM can be larger by an order of magnitude, while in the a2HDM the enhancement is more likely a factor of a few. Unfortunately, the large uncertainties involved in the LECs preclude a more quantitative statement. In the MSSM the situation is more uncertain and $|(d_D - d_n - d_p)/(d_n + d_p)|$ can lie between zero and a factor of a few, depending on the relative sizes of the q(C)EDMs and Weinberg operator. This means that additional tests are required. Such a test could be the following: measurements of d_n, d_p, and d_D allow the extraction of $\bar{g}_1$ from the relation

$$d_D - d_n - d_p = (0.18 \pm 0.023)\bar{g}_1 \, e\,\text{fm} \ . \tag{54}$$

As we shall discuss in the next section, this extraction of $\bar{g}_1$ allows the separation of the $\bar{\theta}$ and mLRSM scenarios from the other two, if measurements of the EDMs of ^{3}He and/or ^{3}H can be made.

To conclude, it is likely that measurements of d_n, d_p, and d_D would allow to disentangle the $\bar{\theta}$ term from the three BSM scenarios discussed here. This already shows the potential impact of the plans to measure d_p and d_D in storage-ring experiments. Unfortunately, the three measurements are most likely not sufficient to disentangle the three BSM scenarios, a problem which is mainly caused by the poor information available on the hadronic $\not{P}\not{T}$ LECs.

4.2 The EDMs of the helion and triton

The experimental EDM storage-ring program not only allows the possible measurement of the proton and deuteron EDMs, but also those of other light nuclei. In particular, measurements on the tri-nucleon EDMs are interesting from the theoretical point of view. These systems are simple enough in order to be accurately described within chiral effective theory, with nuclear uncertainties which are small compared to the hadronic uncertainties in the LECs. In addition, the tri-nucleon EDMs are complementary to the dEDM, mainly due to their much larger dependence on $\bar{g}_0$.

The ^{3}He EDM was calculated using phenomenological PT-even NN potentials (including the Coulomb potential) and a one-meson-exchange model for the $\not{P}\not{T}$ NN potential in Ref. [141] (for older work, see Ref. [142]), while the no-core shell model was used to obtain the nuclear wave function. This framework was also applied in Ref. [50], where the $\not{P}\not{T}$ potential was derived within chiral effective field theory, and results for the ^{3}H EDM were also presented. In a recent work, the authors of [140] used phenomenological PT-invariant potentials in combination with a one-meson-exchange $\not{P}\not{T}$ potential, while Faddeev equations were used to solve the three-body problem. The results of Refs. [50, 141] and [140] on the dependence of the tri-nucleon EDMs on the nucleon EDMs agree. However, in Ref. [140] the dependence on $\bar{g}_{0,1}$ was found to be smaller by a factor two. This discrepancy was recently solved in Refs. [54, 55] which confirmed the smaller results of [140] for $\bar{g}_0$ and $\bar{g}_1$. Thus, the following results apply:

$$\begin{aligned} d_{^3\text{He}} &= \ (0.89 \pm 0.01)\, d_n - (0.039 \pm 0.01)\, d_p + \big[(0.099 \pm 0.026)\, \bar{g}_0 + (0.14 \pm 0.028)\, \bar{g}_1\big]\, e\,\text{fm} \ , \\ d_{^3\text{H}} &= -(0.051 \pm 0.01)\, d_n + (0.87 \pm 0.01)\, d_p - \big[(0.098 \pm 0.024)\, \bar{g}_0 - (0.14 \pm 0.028)\, \bar{g}_1\big]\, e\,\text{fm} \, , \end{aligned} \tag{55}$$

with a nuclear uncertainty of the two-body contributions of approximately 25%. The larger uncertainty compared to the deuteron case arises from the more complicated 3-body Faddeev calculations, where about 20 intermediate partial waves need to be summed in order to reach a stable result for the two-nucleon contribution [54, 55]. The uncertainty of the dependence on the single-nucleon EDMs is much smaller and will be neglected below.

In principle, the tri-nucleon EDMs also depend on the $\not{P}\not{T}$ contact interactions of Eq. (47). However, for the $\bar{\theta}$ term [51,136] and the mLRSM [40] these terms only appear at next-to-next-to-leading order, and can be neglected. In the a2HDM and MSSM they are larger because of the Weinberg operator [50], but also here their contributions turn out to be small compared to pion-exchange contributions. We discuss in this more detail in Sect. 4.2.3.

Finally, the tri-nucleon EDMs could depend on the three-pion vertex proportional to $\bar{\Delta}^{\rm LR}$ which appears at leading order for the mLRSM (see Eq. (32)). This vertex induces a $\not{P}\not{T}$ three-body interaction which, by the power-counting rules of chiral EFT, formally contributes at leading order [40]. However, this term has not been taken into account in any calculation so far. It is therefore unclear whether or not it plays an important role.

4.2.1 The $\bar{\theta}$ term

As was the case for the dEDM, the tri-nucleon EDMs can be expressed in terms of $\bar{\theta}$ with controlled uncertainty. We insert Eqs. (26), (27), and (39) into Eq. (55) and find

$$\begin{aligned} d^{\bar{\theta}}_{^3\mathrm{He}} &= \big[(-2.6 \pm 0.80) - (1.78 \pm 0.70 \pm 0.46) + (0.42 \pm 0.28 \pm 0.08)\big] \cdot 10^{-16}\,\bar{\theta}\,e\,\mathrm{cm}\ , \\ d^{\bar{\theta}}_{^3\mathrm{H}} &= \big[\ \ (1.1 \pm 0.96) + (1.74 \pm 0.68 \pm 0.44) + (0.42 \pm 0.28 \pm 0.08)\big] \cdot 10^{-16}\,\bar{\theta}\,e\,\mathrm{cm}\ , \end{aligned} \tag{56}$$

where the first term in bracket denotes the nucleon EDM contribution, while the second and third term is, respectively, the two-body term due to $\bar{g}_0^{\bar{\theta}}$ and $\bar{g}_1^{\bar{\theta}}$. Just as in Eq. (49) the first error is the hadronic uncertainty, while the second error in the two-body contributions is the nuclear uncertainty. Despite the increase of the latter with respect to the deuteron case, the hadronic uncertainties are still dominant. This might change once more precise lattice results are available, see the discussion in Sect. 6.3.

It is useful to combine the two-body terms into one expression:

$$\begin{aligned} d^{\bar{\theta}}_{^3\mathrm{He}} &= \big[(-2.6 \pm 0.80) - (1.36 \pm 0.88)\big] \cdot 10^{-16}\,\bar{\theta}\,e\,\mathrm{cm}\ , \\ d^{\bar{\theta}}_{^3\mathrm{H}} &= \big[\ \ (1.1 \pm 0.96) + (2.16 \pm 0.85)\big] \cdot 10^{-16}\,\bar{\theta}\,e\,\mathrm{cm}\ . \end{aligned} \tag{57}$$

Several conclusions can be drawn from these relations. First of all, both for the ^{3}He and ^{3}H EDMs the two-body contributions add constructively to the one-body contributions. Second, in both cases the two-body contributions are, within the uncertainties, of similar magnitude as the one-body contributions. Third, measurements of d_n, d_p, d_D, $d_{^3\mathrm{He}}$ and/or $d_{^3\mathrm{H}}$ allow for a relatively precise test of the relevance of the $\bar{\theta}$ term, even without relying on any lattice results. That is, the value of $\bar{\theta}$ can be extracted from $(d_D - d_n - d_p)$, which can then be compared with the predictions

$$\begin{aligned} d_{^3\mathrm{He}} - 0.89\,d_n + 0.039\,d_p &= -(1.36 \pm 0.88) \cdot 10^{-16}\,\bar{\theta}\,e\,\mathrm{cm}\ , \\ d_{^3\mathrm{H}} + 0.051\,d_n - 0.87\,d_p &= \ \ (2.16 \pm 0.85) \cdot 10^{-16}\,\bar{\theta}\,e\,\mathrm{cm}\ . \end{aligned} \tag{58}$$

Of course, using lattice data would allow for additional nontrivial tests.

4.2.2 The mLRSM scenario

Within the mLRSM, the analysis of the tri-nucleon EDMs is very similar to that of the dEDM. Because of the smallness of $\bar{g}_0^{\rm LR}/\bar{g}_1^{\rm LR}$, the terms proportional to $\bar{g}_0$ in Eq. (55) can be neglected. The estimates in Eqs. (29) and (41) then tell us that the tri-nucleon EDMs are, just as the dEDM, about an order of magnitude larger than the nucleon EDMs. In particular, assuming that the nucleon EDM contribution can be neglected at leading order, the mLRSM predicts

$$d_{^3\mathrm{He}}^{\rm LR} \simeq d_{^3\mathrm{H}}^{\rm LR} \simeq 0.7\, d_D^{\rm LR} \ . \tag{59}$$

That is, in this scenario these dipole moments have the same sign and are of the same order of magnitude.

Two caveats exist that could alter this prediction. First of all, the ratio of the two-body-to-one-body contributions has been estimated by NDA. It is not impossible that the nucleon EDM contributions are more important than NDA suggests. A better test then would be to extract $\bar{g}_1$ from $(d_D - d_n - d_p)$ and use this to predict $(d_{^3\mathrm{He}} - 0.89 d_n + 0.039 d_p)$ and/or $(d_{^3\mathrm{H}} + 0.051 d_n - 0.87 d_p)$. However, even this prediction might be altered by the second caveat which consists of possible contributions to the tri-nucleon EDMs proportional to the three-pion vertex $\bar{\Delta}^{\rm LR}$ in Eq. (32). If these contributions are significant, both tests described above will fail because the tri-nucleon EDMs depend on an independent LEC which does not appear in the leading-order expressions of the nucleon and deuteron EDMs[17]. We conclude that a calculation of the dependence on the tri-nucleon EDMs on $\bar{\Delta}^{\rm LR}$ is an important open problem.

4.2.3 The a2HDM and MSSM scenarios

The analysis of the tri-nucleon EDMs within the a2HDM is more complicated than in the previous two scenarios. Similar to the dEDM, the tri-nucleon EDMs are most likely larger than the nucleon EDMs by a factor of a few. However, the exact size of $d_{^3\mathrm{He},^3\mathrm{H}}^{\rm H}/d_{n,p}^{\rm H}$ is uncertain.

In addition, even with measurements of d_n, d_p, and d_D, the tri-nucleon EDMs cannot be firmly predicted. This can be understood from the $\bar{g}_0$ terms in Eq. (55) which are expected to be significant in the a2HDM scenario, but the size of $\bar{g}_0$ cannot be obtained from d_n, d_p, and d_D. One could then think of a negative test: measurements of d_n, d_p, and d_D allow the extraction of $\bar{g}_1$. This value, in combination with d_n and d_p, can be used to predict the tri-nucleon EDMs. If these predictions would not agree with the data, it would indicate that the tri-nucleon EDMs obtain an independent contribution, suggesting that $\bar{g}_0$ plays a role which would hint at the a2HDM. A caveat is that such a scenario could also point to the mLRSM in which the independent contribution is due to $\bar{\Delta}^{\rm LR}$.

A better method to test the a2HDM scenario then seems to be the following: from measurements of d_n, d_p, and d_D, it is possible to extract the size of $\bar{g}_1^{\rm H}$. This value, in combination with a measurement of $d_{^3\mathrm{He}}$ ($d_{^3\mathrm{H}}$), allows for the extraction of $\bar{g}_0^{\rm H}$. The value of $d_{^3\mathrm{H}}$ ($d_{^3\mathrm{He}}$) can then be predicted.

Lattice calculations could improve this somewhat bleak scenario where five EDMs are necessary for a proper test. Because in the a2HDM, the nucleon EDMs depend on the EDM and CEDM of the d quark and on the Weinberg operator, lattice calculations of the nucleon EDM will be very difficult. On the other hand, the $\not{P}\not{T}$ pion-nucleon LECs mainly depend on the qCEDM.

[17] It should be noted that $\bar{\Delta}^{\rm LR}$ is expected to contribute to the dEDM at next-to-leading order [40]. However, its precise contribution has not been calculated so far.

If $\bar{g}_{0,1}$ can be calculated as a function of the qCEDM, the number of necessary experiments can be reduced.

If in case of the MSSM the qCEDM turns out to be significant the pattern of tri-nucleon EDMs would be similar to that of the a2HDM. That is, the tri-nucleon EDMs are expected to depend on $\bar{g}_0$ as well. However, if the qEDM and/or Weinberg operator dominate the qCEDM, $d_{^3\mathrm{He}}$ ($d_{^3\mathrm{H}}$) are expected to lie close to d_n (d_p).

Finally we comment on the $\not{P}\not{T}$ contact LECs in Eq. (47). As discussed in Refs. [50, 136], for most $\not{P}\not{T}$ dimension-four and -six operators these terms are very small. For the Weinberg operator, however, which appears in the a2HDM and MSSM scenarios, these operators could be as important as one-pion exchange between nucleons involving $\bar{g}_0$. As we argued in Sect. 3.1.3, in the a2HDM the contribution from the Weinberg operator to $\bar{g}_0$ can be neglected, because of the larger contribution from the down-quark CEDM. This implies that the contributions from the interactions in Eq. (47) to the $\not{P}\not{T}$ NN potential can be neglected as well. In addition, Ref. [50] found that the dependence of the tri-nucleon EDMs on $\bar{C}_{1,2}$ was smaller then expected by power counting. This last point could imply that also in the MSSM it is safe to neglect the $\not{P}\not{T}$ nucleon-nucleon contact interactions in the tri-nucleon EDMs. However, the contact interactions might become more important in heavier nuclei.

4.3 Tri-nucleon EDMs: an overview

For probing the QCD $\bar{\theta}$ term the tri-nucleon EDMs are very promising observables. Because the tri-nucleon EDMs depend on $\bar{g}_0$ at leading order, the two-body contributions are a few times bigger than for the deuteron EDM which implies that the tri-nucleon EDMs are not dominated by the constituent nucleon EDMs. The EDMs of the helion and trition are thus expected to be larger than the EDMs of the neutron and proton. Furthermore, the small nuclear uncertainties allow for a proper test of strong CP violation, once $\bar{\theta}$ has been determined from measurements of d_n, d_p, and d_D, or from lattice calculations in combination with a measurement of d_n and/or d_p.

Measurements of the tri-nucleon EDMs would also provide important information on the mLRSM scenario. In particular, the $\not{P}\not{T}$ two-body interactions dominate over the nucleon EDMs by an order of magnitude, as in the case of the deuteron EDM. If this were the whole story, this would imply that d_D, $d_{^3\mathrm{H}}$, and $d_{^3\mathrm{He}}$ depend only on a single LEC $\bar{g}_1^{\mathrm{LR}}$ which means that once one of these EDMs has been measured, the other two can be predicted. However, the tri-nucleon EDMs might obtain an important contribution from the three-pion vertex proportional to $\bar{\Delta}^{\mathrm{LR}}$. A more conclusive statement can be made once the dependence of the tri-nucleon EDMs on $\bar{\Delta}^{\mathrm{LR}}$ has been calculated.

In the a2HDM scenario, the tri-nucleon EDMs are in principle independent from the deuteron EDM because of the dependence on $\bar{g}_0^H$. Estimates of the nucleon EDMs and the pion-nucleon LECs $\bar{g}_{0,1}^{\mathrm{H}}$ suggest that the two-body contributions dominate the light-nuclear EDMs – however, the uncertainties are large. A lattice calculation of the $\bar{g}_{0,1}^{\mathrm{H}}$ induced by the qCEDM could significantly improve the situation. A lattice calculation of $d_{n,p}$ would be beneficial as well, but more complicated because of its dependence on the three BSM operators in Eq. (21).

Depending on the hierarchy between the BSM operators in Eq. (24), the situation in the MSSM might be very close to the a2HDM. This implies that these scenarios cannot be disentangled using light-nuclear EDMs alone. On the other hand, if in the MSSM the qEDMs or the Weinberg operator are significantly larger than the qCEDMs, this would imply that $\not{P}\not{T}$

two-body effects in light-nuclear EDMs are relatively small compared to contributions from the nucleon EDMs. In this particular, and admittedly *ad hoc*, case, the EDMs of the deuteron and tri-nucleon EDMs should be well approximated by their constituent nucleon EDMs. Thus, the MSSM might leave a footprint behind in the hierarchy of light-nuclear EDMs which is distinct from the other scenarios.

In any case, measurements of the tri-nucleon EDMs would provide important information on the source of non-KM *CP* violation, if such a source exists. Measurements of the nucleon, deuteron, and tri-nucleon EDMs allow one to disentangle the $\bar{\theta}$ and mLRSM scenarios from the a2HDM and MSSM scenarios considered in this paper. It is in general not possible to separate the latter two from each other using light-nuclear EDM measurements alone.

5 EDMs of other systems

In this section we briefly discuss EDMs of other systems which are not the main focus of this work. In particular we consider, within the above scenarios, $\not{P}\not{T}$ effects in the paramagnetic atom/molecules ^{205}Tl, YbF, and ThO, which depend on the electron EDM (eEDM) and semi-leptonic four-fermion operators. We also discuss the EDM of the diamagnetic ^{199}Hg atom. There exist strong experimental limits on these EDMs, but atomic and nuclear theory is required to relate the existing experimental bounds on T-violating effects in these complicated systems to an underlying mechanism of *CP* violation.

5.1 The EDMs of paramagnetic systems

So far we have focused on hadronic EDMs, but the electron EDM is, of course, an important observable as well. In general, eEDM measurements are complementary to hadronic EDM measurements because they probe different fundamental parameters. The eEDM, however, is not measured directly but inferred from measurements on atomic and molecular systems. The current strongest bound on the eEDM comes from the limit on a T-violating effect in the molecule ThO [15]. Strong limits are obtained from the molecule YbF [143, 144] and the paramagnetic atom ^{205}Tl [145] as well. The eEDM is not the only $\not{P}\not{T}$ source that would generate an EDM of ^{205}Tl or the T-violating effects searched for in YbF and ThO. In particular, additional contributions can arise from $\not{P}\not{T}$ semi-leptonic four-fermion operators, but, as discussed below, these contributions can be neglected as compared to the one due to the electron EDM.

In the $\bar{\theta}$ scenario, that is to say, in the SM with massless neutrinos and a nonzero $\bar{\theta}$ term, the eEDM is generated as a spill-over from the quark sector by the $\bar{\theta}$ term and the KM phase and is therefore much smaller than the EDM of a nucleon [146–148], $|d_e| \lesssim 10^{-37}\, e$ cm. Contributions from $\not{P}\not{T}$ semi-leptonic interactions to T-violating effects in atoms and molecules might be larger than those from the eEDM, but also they are strongly suppressed [149]. Therefore, in the $\bar{\theta}$ scenario we do not expect a nonzero measurement of a T-violating effect in the above paramagnetic systems.

In the mLRSM, both the qEDMs and the eEDM are generated at one-loop. These expressions differ because the diagram for the qEDM involves quarks whereas in the case of the eEDM the loop involves massive neutrinos. The qEDMs d_u and d_d involve the factor $\sum_{i=d,s,b} \mathrm{Im}(e^{-i\alpha} m_i V_L^{ui} V_R^{ui*})$ and $\sum_{j=u,c,t} \mathrm{Im}(e^{-i\alpha} m_j V_L^{jd} V_R^{jd*})$, respectively [69, 150, 151], while the expression for the electron EDM contains the factor $\mathrm{Im}(e^{-i\alpha}(M_{\nu_D})_{ee})$ [152, 153], where M_{ν_D}

is the neutrino Dirac-mass matrix. Because the expressions for d_q and d_e involve different parameters their relative magnitudes cannot be reliably compared in general. However, if we assume the *CP* phases in both cases to be of the same order and take the *ee* element of the neutrino Dirac-mass matrix to be of the of order the electron mass, $|M_{\nu_D}| \simeq m_e$, the eEDM will be suppressed with respect to the qEDM by at least a factor $m_e/m_{u,d}$. Since, in the mLRSM, the qEDM make negligible contributions [69] to hadronic and nuclear EDMs as compared to the dominant contribution of the tree-level generated four-quark operator discussed in Sect. 2.2, the eEDM is expected to be significantly smaller than the nEDM. Assuming $|M_{\nu_D}| \simeq m_e$ and the different phases to be of the same order, we estimate $d_e/d_n \sim 10^{-4}$. We emphasize that a more precise statement is not possible because the hadronic and electron EDMs depend on different parameters.

In the version of the a2HDM discussed in Sect. 2.3 the contribution to the eEDM is dominated by two-loop diagrams and the expressions are nearly identical to those of the d-quark EDM. Two things are altered. First of all, there is the obvious difference between the masses and charges of the d quark and the electron. More important is that the eEDM depends on a different *CP*-odd parameter, namely, $\mathrm{Im}(\varsigma_l \varsigma_u^*)$ where ς_l is defined analogously to ς_d [61], *cf.* Eq. (15). This means it will be hard to compare the d-quark EDM and eEDM in general. If we assume the two *CP*-violating parameters to be of the same order, the magnitudes of the two EDMs should be comparable at the electroweak scale with a minor enhancement of the d-quark EDM by a factor m_d/m_e. However, the d-quark EDM gets large contributions from the d-quark CEDM when the operators are evolved to lower energies. It is more interesting to look at the electron-to-neutron-EDM ratio in the a2HDM. Assuming the *CP*-violating parameters to be equal (see Eq. (76)) and using Eq. (46) we estimate $|d_e/d_n| \sim 10^{-2}$. The upper bound on the eEDM then implies a bound on the nEDM $d_n \lesssim 10^{-26}\, e\,\mathrm{cm}$ in this scenario. In view of the dependence of the eEDM and nEDM on different parameters this bound is not very stringent.

In the MSSM one expects, in general, the electron-to-neutron-EDM ratio to be of the same order of magnitude as in the a2HDM. In particular, the 'split SUSY' scenario predicts a strong correlation between these EDMs, $|d_e/d_n| \sim 1/10$ [111], up to theoretical uncertainties in the calculation of d_n.

What about the semi-leptonic operators in the BSM scenarios? In both the mLRSM and the a2HDM they are generated through tree-level exchange of a heavy Higgs boson. These operators are therefore suppressed by a factor $m_q m_e/v^2$ from the Yukawa couplings. In addition there is a factor $1/m_H^2$ from Higgs-boson exchange H, where m_H denotes the mass of H. While in the a2HDM m_H must not exceed ~ 1 TeV, in the mLRSM the masses of the heavy Higgs bosons with *CP*-violating Yukawa couplings are of the order of 10 TeV.

Even though in both models the eEDM is generated at the loop level, it nevertheless dominates the contributions to the above atomic/molecular T-odd effects. The only way around this is if the *CP* phases that appear in d_e are tuned to be much smaller than the phases of the coefficients of the semi-leptonic operators. Barring this possibility then, in the a2HDM, the contributions from the semi-leptonic operators to the T-violating effects in ^{205}Tl, ThO, and YbF are suppressed by about two orders of magnitude with respect to those of the eEDM, see Ref. [62] for a more detailed discussion. In the mLRSM the contributions of the $\not{P}\not{T}$ semi-leptonic operators to these paramagnetic systems are even less important than in the a2HDM, in view of the larger suppression factors discussed above. In the MSSM, the $\not{P}\not{T}$ semi-leptonic operators are non-negligible, especially when the first and second generation of sfermions are very heavy [93]. However, because global fits to experimental data seem to disfavor large values of $\tan\beta \gtrsim 30$

(*cf.* Sect. 2.4), the dominant contribution to, e.g., the ^{205}Tl EDM still comes from the electron EDM [93]. Thus one may conclude that the eEDM provides the dominant contribution to the T-violating effects in ^{205}Tl, ThO, and YbF.

In summary, the size of the eEDM with respect to hadronic EDMs gives additional information to disentangle the various scenarios. Clearly, a nonzero eEDM would rule out the pure $\bar{\theta}$-scenario. Within the a2HDM and the MSSM, the eEDM is expected to be about one to two orders of magnitude smaller than the neutron EDM. In the mLRSM this suppression is expected to be even larger. However, in these scenarios no solid predictions can be made because the eEDM and the hadronic EDMs depend, in general, on different unknown parameters.

5.2 The ^{199}Hg EDM

Schiff's theorem [154] ensures that in the non-relativistic limit the EDM of a point-like nucleus in an atomic system is completely screened by the electrons surrounding the nucleus. This would imply that the total EDM of an atomic system is zero. However, in real atoms the necessary conditions for Schiff's theorem to apply are violated. For example, in case of ^{199}Hg, a diamagnetic atom, the largest contribution to the atomic EDM stems from the finite size of the nucleus and is induced by the so-called nuclear Schiff moment S_{Hg}[18]. For ^{199}Hg, the relation between the atomic EDM, d_{Hg}, and S_{Hg} is given by [12, 155–157]

$$d_{\mathrm{Hg}} = (2.8 \pm 0.6) \cdot 10^{-4}\, S_{\mathrm{Hg}}\, \mathrm{fm}^{-2} \ , \tag{60}$$

with an uncertainty estimate based on Ref. [158]. While the atomic calculation is rather well under control, the main uncertainties arise from the nuclear-theory calculation of S_{Hg}. Typically it is calculated as a function of the pion-nucleon couplings, *cf.* Eq. (25), and the single nucleon EDMs. However, at present there exists no EFT for nuclei with this many nucleons. It is therefore not clear whether or not there will be important contributions from other $\not{P}\not{T}$ hadronic interactions such as the contact interactions in Eq. (47). In addition, corrections to leading terms cannot be systematically calculated which means that the uncertainties are difficult to quantify. If we assume that S_{Hg} is dominated by pion-nucleon interactions, the estimated uncertainties are large [12, 52, 159]

$$S_{\mathrm{Hg}} = [(0.37 \pm 0.3)\bar{g}_0 + (0.40 \pm 0.8)\bar{g}_1]\ e\,\mathrm{fm}^3 \ . \tag{61}$$

For example, in case of the $\bar{\theta}$ scenario we can use Eqs. (26) and (27) to obtain[19]

$$S_{\mathrm{Hg}}^{\bar{\theta}} = [-(6.5 \pm 2.5 \pm 5.3) + (1.2 \pm 0.8 \pm 2.4)] \cdot 10^{-3}\, \bar{\theta}\, e\,\mathrm{fm}^3 \ , \tag{62}$$

with the first term due to $\bar{g}_0^{\bar{\theta}}$ and the second due to $\bar{g}_1^{\bar{\theta}}$. In each bracket the first error is the hadronic uncertainty from the coupling constants and the second the nuclear uncertainty taken from Eq. (61). In contrast to the results for the EDMs of light nuclei, here the nuclear

[18] The mercury EDM also receives contributions from the electron EDM and $\not{P}\not{T}$ semi-leptonic interactions, but these are better probed in the paramagnetic systems discussed in the previous section. We therefore do not discuss the (semi-)leptonic contributions here.

[19] In case of the $\bar{\theta}$ term, $S_{\mathrm{Hg}}^{\bar{\theta}}$ receives contributions from the nucleon EDMs which are of the same order as the $\bar{g}_{0,1}^{\bar{\theta}}$ contributions [158]. We do not give the detailed expressions here.

uncertainty is dominant and might be difficult to reduce. Inserting Eq. (62) into Eq. (60) and combining all uncertainties gives

$$d_{\rm Hg}^{\bar\theta} = -\,(1.5 \pm 1.8)\cdot 10^{-19}\,\bar\theta\,e\,{\rm cm}\ , \tag{63}$$

to which the contributions from the constituent nucleon EDMs still need to be added. This result implies that even if a nonzero EDM was measured for ^{199}Hg, the uncertainties, at the moment, would be too large to test the $\bar\theta$ scenario.

In the mLRSM scenario, the dominant contribution to $S_{\rm Hg}$ is expected to come from $\bar g_1^{\rm LR}$. However, due to the large nuclear uncertainty it is not possible to predict the size of $d_{\rm Hg}$ once $\bar g_1^{\rm LR}$ has been extracted from, for example, light-nuclear EDM experiments. For the same reason a measurement of $d_{\rm Hg}$ cannot be used to extract a sufficiently precise value of $\bar g_1^{\rm LR}$. The discussion for the a2HDM and MSSM[20] scenarios is similar to the mLRSM scenario. In these cases, also $\bar g_0^{\rm H}$ is expected to give a significant contribution, but again the nuclear uncertainties are too large to extract any nontrivial, quantitative information. In conclusion, disentangling the various scenarios using measurements of $d_{\rm Hg}$ is not possible, unless the nuclear theory is improved substantially[21].

6 Discussion, outlook, and summary

6.1 Testing strategies

Based on the findings of this paper there are several strategies to reveal nontrivial information on the $\not{P}\not{T}$ sources, once non-vanishing measurements and/or improved lattice calculations of EDMs of nucleons and light nuclei are available[22].

Since the $\not{P}\not{T}$ pion-nucleon coupling constants are known quantitatively for a non-vanishing $\bar\theta$-term, the most conclusive tests can be formulated for this scenario: if the QCD $\bar\theta$-term is assumed to be the prominent source of CP violation beyond the CKM-matrix, it follows directly from Eq. (56) that the value of $\bar\theta$ can be extracted from EDM measurements of both the neutron and ^{3}He via

$$d_{^3{\rm He}} - 0.9\,d_n = (-1.4 \pm 0.9)\cdot 10^{-16}\,\bar\theta\,e\,{\rm cm}\ , \tag{64}$$

where the uncertainties were added in quadrature and we dropped the contribution from the proton EDM, whose contribution to $d_{^3{\rm He}}$ is strongly suppressed. A lattice calculation for d_n then allows for the first nontrivial test of the assumed scenario. Note that in this case all nonperturbative QCD effects can be controlled quantitatively. In the next subsection we discuss how the present uncertainty of about 70% can be reduced further. The value of $\bar\theta$ extracted from Eq. (64) can now be used to predict

$$d_D - d_n - d_p = (5 \pm 4)\cdot 10^{-17}\,\bar\theta\,e\,{\rm cm}\ , \tag{65}$$

where the uncertainties displayed in Eq. (49) were again added in quadrature. This provides the second nontrivial test, if in addition also the EDM of the deuteron, d_D, and of the proton,

[20] For a recent analysis of Schiff moments within the MSSM, see Ref. [116].

[21] Future experiments on ^{225}Ra might be more promising since the nuclear theory is more reliable than for ^{199}Hg [12].

[22] In this section we do not consider measurements of the EDM of ^{3}H since, due to its radioactive nature, it is not likely to be measured in a storage ring experiment.

d_p, were measured. If the same value of $\bar{\theta}$ could explain simultaneously the measured values of $d_{^3\mathrm{He}}$, d_D as well as d_n and d_p calculated on the lattice, it would provide very strong evidence that indeed the QCD $\bar{\theta}$-term is the origin of the non-vanishing EDMs.

If the QCD $\bar{\theta}$-term would not pass this test, alternative scenarios need to be studied. In this work we considered, for illustration, the mLRSM, the a2HDM, and the MSSM. In these cases the absence of a quantitative knowledge of the induced LECs hinders predictions for the nuclear EDMs analogous to Eqs. (64) and (65). However, at least for the mLRSM different EDMs can be related to each other, since in this scenario $\bar{g}_1$ dominates over $\bar{g}_0$. This results in the prediction that the single nucleon EDM should be significantly smaller than the nuclear ones. In addition, one may extract $\bar{g}_1^{\mathrm{LR}}$ from Eq. (48)

$$d_D - (d_n + d_p) \simeq d_D = (0.18 \pm 0.02)\, \bar{g}_1^{\mathrm{LR}} e\,\mathrm{fm}\ .$$

This value of $\bar{g}_1^{\mathrm{LR}}$ can then be used to predict $d_{^3\mathrm{He}}$ according to Eq. (55)

$$d_{^3\mathrm{He}} - 0.9\, d_n \simeq d_{^3\mathrm{He}} = (0.14 \pm 0.03)\, \bar{g}_1^{\mathrm{LR}}\, e\,\mathrm{fm}\ .$$

Note, this nice relation could be spoiled by a potentially large *CP*-odd three-body force, as discussed above. If the mLRSM fails its test, too, the physics responsible for the *CP*-violation must come from yet another theory beyond the Standard Model, candidates being the a2HDM and the MSSM discussed in this work: in these models $\bar{g}_0$ and $\bar{g}_1$ are expected to be similar in size and the single-nucleon as well as ^{3}He EDMs acquire additional important contributions. As outlined in Sect. 5.1 the electron EDM might provide additional information to disentangle the mLRSM from the other scenarios.

Thus, if the EDMs for proton, neutron, deuteron, and ^{3}He were measured with high precision, highly nontrivial information could be deduced on the *CP*-violating physics responsible for their appearance.

6.2 Expected sensitivities

So far we have focused on ways to disentangle the four scenarios of *CP* violation. However, it is also interesting to see how well the current and proposed EDM experiments are able to probe non-KM *CP* violation in each of the four scenarios. To this end we will discuss the sensitivities to the *CP*-violation parameters that would result from EDM measurements of the proton, deuteron, and helion at the envisaged accuracy [16–19]. These sensitivities are shown in Table 1 for the $\bar{\theta}$ and mLRSM scenarios and in Fig. 4 for the a2HDM scenario. We do not discuss the MSSM scenario here. For comparison, we also show the bounds that can be set by the current upper limit on the neutron EDM [5]. The most conservative values allowed by the uncertainties of the expressions in Sects. 3 and 4 were used to obtain these bounds and sensitivities. We assigned an uncertainty of a factor 10 to the estimates based on NDA.

The current upper limit on the neutron EDM already stringently constrains the *CP*-violating parameters appearing in each of the three scenarios[23]. Obviously, for all scenarios a measurement of the proton EDM at the proposed accuracy would greatly improve the sensitivity to the *CP*-violating parameters as compared to the current neutron EDM limit.

[23]The bound on the *CP*-violating parameters of the mLRSM in Table 1 would be an order of magnitude stronger if we would not include the factor 10 uncertainty assigned to the NDA estimate. Such a bound would still be roughly an order of magnitude weaker than the bound derived in Ref. [60], see Ref. [74] for more details.

	d_n	d_p	d_D	$d_{^3\mathrm{He}}$
$\bar{\theta}$	$1 \cdot 10^{-10}$	$\times$	$\times$	$4 \cdot 10^{-14}$
$\sin\zeta\,\mathrm{Im}(V_L^{ud*} V_R^{ud} e^{i\alpha})$	$4 \cdot 10^{-5}$	$2 \cdot 10^{-8}$	$2 \cdot 10^{-9}$	$2 \cdot 10^{-9}$

Table 1: Sensitivities to the magnitudes of *CP*-violating parameters of the $\bar{\theta}$ and mLRSM scenarios. The first column shows the relevant parameters, while the second column shows bounds from the current upper limit on the neutron EDM, $d_n \leq 2.9 \cdot 10^{-26} e\,\mathrm{cm}$. The remaining columns show the values to which the *CP*-violating parameters could be probed by measurements of the proton, deuteron, and helion EDMs at the envisaged accuracy: 10^{-29} e cm. The contributions of $\bar{\theta}$ to the proton and deuteron EDMs are consistent with zero within the uncertainties of Eqs. (39) and (49) and can therefore, at the moment, not be used to probe $\bar{\theta}$. If we were to take the central values of Eqs. (39) and (49), we would obtain sensitivities of $9 \cdot 10^{-14}$ and $8 \cdot 10^{-14}$ for d_p and d_D, respectively.

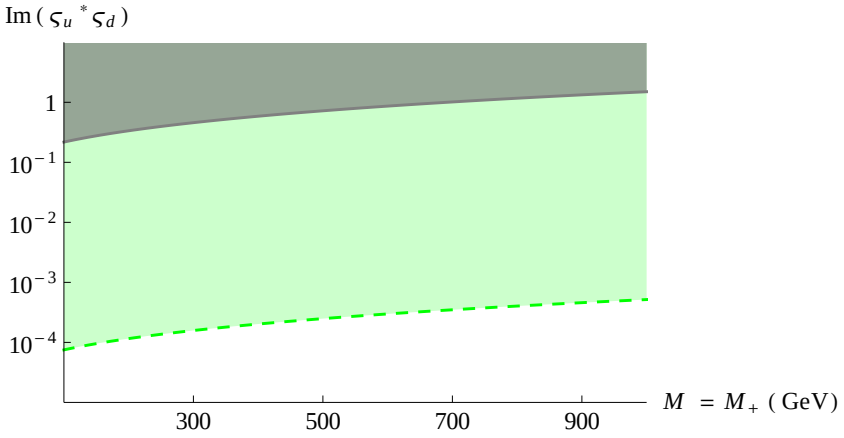

Figure 4: Sensitivities to the magnitude of the *CP*-violating parameter $\mathrm{Im}(\varsigma_u^* \varsigma_d)$ as a function of the mass of the additional Higgs fields. The region of parameter space which is excluded by the current upper limit on the neutron EDM ($d_n \leq 2.9 \cdot 10^{-26}\,e\,\mathrm{cm}$) is shown in grey and bounded by the solid line. The region that would be probed by a measurement of the proton EDM at the accuracy of 10^{-29} e cm is shown in green and bounded by the dashed line.

To what extent the deuteron and/or helion EDMs are more sensitive than the proton EDM depends on the relative sizes of the corresponding EDMs which differ between the various scenarios. In the $\bar{\theta}$ scenario, the helion EDM should be a few times bigger than the deuteron and proton EDMs, while in the mLRSM scenario both the deuteron and helion EDMs are expected to be an order of magnitude larger than the proton EDM. This is reflected in Table 1, where the greatest sensitivity to $\bar{\theta}$ would come from a helion EDM measurement, while a deuteron EDM measurement would be the best probe for the mLRSM scenario. In the a2HDM scenario, the deuteron and helion EDMs are expected to be of similar size, both are larger than the proton EDM by a factor of a few. However, the exact size of this factor is rather uncertain and we therefore only show in Fig. 4 the region of parameter space which could be probed by a measurement of the proton EDM at an accuracy of $10^{-29} e\,\mathrm{cm}$.

6.3 How to improve the theoretical accuracy

Various paths are possible to improve the theoretical accuracy of the EDM calculations and make, in this way, the tests outlined in Sect. 6.1 even more challenging for the models.

Let us first consider *CP* violation due to the QCD $\bar{\theta}$-term. An improved theoretical understanding of single-nucleon EDMs can come from lattice QCD only. Respective calculations near or even at the physical pion mass including the still missing estimates of the pertinent systematic errors are necessary. In this way the parameter $\bar{\theta}$ could be determined from a measurement of, e.g., the neutron EDM and used to predict the EDMs of the proton and the light nuclei based on Eqs. (64) and (65).

The uncertainties of the two-nucleon contributions are dominated by those of the coupling constants, i.e., the nuclear part of the calculations is sufficiently well under control. This is clearly visible in the deuteron result Eq. (49), where the nuclear uncertainty is only about 15% of the hadronic one. For the helion and triton calculations the nuclear uncertainty increases to about 60% of the hadronic one, *cf.* Eq. (56).

To reduce the uncertainties of the $\not{P}\not{T}$ pion-nucleon coupling constants $\bar{g}_0^\theta$ and $\bar{g}_1^\theta$, *cf.* Eqs. (26) and (27), respectively, again lattice QCD may play an important role. About half of the uncertainty of $\bar{g}_0^\theta$ results from the QCD contribution to the neutron-proton mass difference, the other half from the ratio of the u to d quark masses. In the last ten years the determination of the latter quantity has improved from a range of 0.3–0.7 (*cf.* Ref. [160]) to 0.38–0.58 (*cf.* Ref. [63]) because of improved lattice QCD calculations. The standard for lattice calculations is now "full QCD" with two light (u and d sea) quarks plus one heavy (s sea) quark [161,162]. Direct lattice determinations exist already for the strong-interaction contribution to the neutron-proton mass difference [163] which will be improved in the future. In addition, once the electromagnetic contribution to hadronic ground state masses can be fully included in the simulations (see Ref. [164] for the state of the art which, however, does not include all dynamical effects yet), the physical neutron-proton mass difference can be included in the analysis as well which should lead to improved values of both m_u/m_d and the strong-interaction contribution to the neutron-proton mass difference. This in turn will lead to a reduction of the uncertainty of $\bar{g}_0^\theta$.

The situation for $\bar{g}_1^\theta$ is different to the extend that only half of the uncertainty given in Eq. (27) stems from the LEC c_1. This LEC is related to the nucleon σ-term and is open for improvements from lattice QCD or from studies of the πN-system. The other half results from the NDA estimate of an additional contribution to the isospin-breaking $\not{P}\not{T}$ pion-nucleon vertex which cannot be traced back to the σ-term. In summary, future lattice calculations might reduce the uncertainty of $\bar{g}_1^\theta$ listed in Eq. (27) by a factor of two, such that the two-nucleon contribution to the deuteron EDM, the analog of Eq. (50), will be predicted with only a (30–40)% error.

Even the comparably small nuclear uncertainty can be reduced by about a factor of two by replacing the PT-even N^{2}LO interactions and pertinent wave functions by their N^{3}LO counterparts (including N^{3}LO three-body forces in the helion and triton cases) [54,55]. The application of these improved chiral potentials and wave functions together with the envisaged lattice improvements might finally reduce the uncertainties of the two-nucleon contributions to the helion and triton EDMs listed in Eq. (58) to a (20–30)% error.

The improvements in the chiral potentials and wave functions hold of course also for the BSM scenarios. The uncertainty of the two-nucleon contribution to the deuteron EDM (Eq. (48)) and to the tri-nucleon EDMs (Eq. (55)) might then be reduced by about 50%. Nevertheless the biggest unknowns in these cases are the hadronic inputs, the LECs $\bar{g}_0$ and $\bar{g}_1$ (and, in addition,

the strength of the three–pion vertex, $\bar{\Delta}$, in the mLRSM scenario). The calculation of the $\not{P}\not{T}$ three-point correlators, pion-two-nucleon for $\bar{g}_{0,1}$ and three-pion for $\bar{\Delta}$, seems to be a task that probably only lattice calculations can address in the future. The same can be said of the single-nucleon EDMs generated by dimension-six sources.

6.4 Summary

In this work we have investigated, by using four different models of flavor-diagonal *CP* violation, how distinct *CP* scenarios leave their footprint in EDMs of different systems. Such a study has to be performed in several steps: First, the models are analyzed at some high-energy scale where perturbation theory applies. We studied the Standard Model (with massless neutrinos) including the QCD $\bar{\theta}$ term, the minimal left-right symmetric model (mLRSM), an aligned two-Higgs model (a2HDM) and, briefly, the minimal supersymmetric extension of the Standard Model (MSSM). In each case we have investigated the pertinent *CP*-odd sources and how they induce, at lower energies, effective $\not{P}\not{T}$ operators of dimension six (in the Standard Model case, the $\bar{\theta}$ term appears directly and is of dimension four). Because symmetries and field content differ between the four scenarios, they give rise to different (sets of) effective operators. In the Standard Model the only relevant operator is the $\bar{\theta}$ term, in the mLRSM the dominant operator is a $\not{P}\not{T}$ four-quark operator with nontrivial chiral and isospin properties, while in the a2HDM scenario the quark EDM, chromo-EDM, and the Weinberg three-gluon operator are all relevant. In the MSSM the situation is, in general, similar to the a2HDM, although distinctive scenarios are also possible within the MSSM framework, *cf.* Sect. 2.4.

The next step involves the evolution of the resulting operators to the low energies where the experiments take place. This can be done perturbatively down to an energy around the chiral-symmetry-breaking scale by use of one-loop QCD renormalization-group equations. To go to even lower energies, nonperturbative techniques are required. In this work we have extended the Lagrangian of chiral perturbation theory (χPT) to obtain an EFT describing $\not{P}\not{T}$ interactions among pions, nucleons, and photons which are the relevant degrees of freedom for hadronic and nuclear EDMs. χPT allows for a systematic derivation of the operator structure of the $\not{P}\not{T}$ hadronic interactions. However, only some low energy parameters induced by the $\bar{\theta}$ term can be controlled quantitatively. For all other scenarios each interaction comes with an unknown strength, traditionally called low energy constant (LEC), whose size cannot be obtained from symmetry arguments alone. Nevertheless, as argued here and elsewhere [39, 40, 51], symmetry considerations still provide important clues on the hierarchy of the various interactions.

It was demonstrated that the $\not{P}\not{T}$ dimension-four and -six operators appearing in the various scenarios transform differently under chiral and isospin rotations which carries over to the parameters of the chiral Lagrangian. In the pionic and pion-nucleon sector the most important interactions are given by

$$\mathcal{L} = \bar{g}_0 \bar{N} \boldsymbol{\pi} \cdot \boldsymbol{\tau} N + \bar{g}_1 \bar{N} \pi_3 N - \bar{\Delta} \frac{\pi_3 \boldsymbol{\pi}^2}{2F_\pi} \ , \tag{66}$$

where the relative sizes of the three LECs $\bar{g}_{0,1}$ and $\bar{\Delta}$ depend crucially on the *CP*-odd scenario under investigation. In particular, one finds for the ratio $\bar{g}_1/\bar{g}_0$ [39, 40, 51, 132]

$$\frac{\bar{g}_1^{\bar{\theta}}}{\bar{g}_0^{\bar{\theta}}} = -0.2 \pm 0.1 \ , \qquad \frac{\bar{g}_1^{\rm LR}}{\bar{g}_0^{\rm LR}} = -50 \pm 25 \ , \qquad \left| \frac{\bar{g}_1^{\rm H}}{\bar{g}_0^{\rm H}} \right| \simeq 1 \ , \qquad \left| \frac{\bar{g}_1^{\rm MSSM}}{\bar{g}_0^{\rm MSSM}} \right| \simeq 1 \ , \tag{67}$$

where the uncertainties are largest in the a2HDM and MSSM scenarios. In addition, the three-pion vertex proportional to $\bar{\Delta}$ only appears at leading order in the mLRSM [40], while it provides a next-to-next-to-leading-order correction in the other scenarios.

Despite these differences in the pionic and pion-nucleon sector, the EDMs of the nucleons do not necessarily show a distinct pattern, since in all scenarios the nucleon EDMs obtain leading-order contributions from the short-range operators of Eq. (35) [42–48]. The sizes of the corresponding LECs are not constrained by chiral symmetry which means that our approach has little predictive power in the single-nucleon sector. Model calculations or estimates can provide some information on the sizes of the LECs, but the uncertainties are large. In case of the $\bar{\theta}$ term, lattice results are available which provide additional information, but, at the moment, the uncertainties are still too large to draw firm conclusions. In summary, measurements of the nucleon EDMs are not enough to disentangle the various scenarios.

Dedicated storage rings might allow for measurements of EDMs of light ions. Because χPT allows for a unified description of nucleons and (light) nuclei, light-nuclear EDMs can be calculated in terms of the LECs in Eq. (66) and the nucleon EDMs. The associated nuclear uncertainties can be systematically estimated and turn out to be small compared to the uncertainties in the sizes of the LECs themselves in contrast to calculations of some of the heavier systems. One reason why the storage ring proposals are so interesting is that nuclear EDMs already depend at tree level on the interactions in Eq. (66), providing direct access to the nontrivial relations of Eq. (67), in contrast to the single-nucleon EDMs, where these interactions contribute only at one-loop level and are masked by the presence of the additional short-ranged operators mentioned above. Since different light-nuclear EDMs[24] depend on the same set of LECs with different relative weight [50], the dependence on $\bar{g}_{0,1}$ (and possibly $\bar{\Delta}$) can be isolated and the hierarchy presented in Eq. (67) can be studied experimentally, once measurements are performed on the EDMs of different light ions as discussed in Sect. 6.1.

It should be stressed that the models discussed in this paper were chosen to illustrate the potential as well as limitations of detailed analyses of various EDM measurements. Clearly, this choice is to some extend arbitrary and does by no means exhaust the possible options for physics beyond the Standard Model. However, it should have become clear that the methods applied in this and earlier works are quite general and can also be used to analyze the signatures of other models for *CP* violation beyond the Kobayashi-Maskawa mechanism.

In summary we have argued that an experimental program aimed at measurements of EDMs of light nuclei is very promising. Such measurements have sufficient sensitivity to probe scales where well-motivated scenarios of physics beyond the Standard Model are expected to appear. In addition, we have demonstrated that these measurements are expected to play an essential role in unraveling the origin(s) of *CP* violation.

Acknowledgements

We thank Daniel Boer, Feng-Kun Guo, Susanna Liebig, Emanuele Mereghetti, David Minossi, Andrea Shindler, Rob Timmermans, and Bira van Kolck for useful discussions. This work is supported in part by the DFG and the NSFC through funds provided to the Sino-German CRC 110 "Symmetries and the Emergence of Structure in QCD" (Grant No. 11261130311). We acknowledge the support of the European Community-Research Infrastructure Integrating

[24] in this work we looked at the deuteron, helion, and triton EDMs, but other light-nuclear EDMs can be calculated in similar fashion.

Activity "Study of Strongly Interacting Matter" (acronym HadronPhysics3, Grant Agreement n. 283286) under the Seventh Framework Programme of EU.

A The minimal left-right symmetric model

In this appendix we discuss the $\not{P}\not{T}$ dimension-six operators arising in the mLRSM that can contribute to Eq. (1). In particular we derive the operator in Eq. (8) which gives the dominant contribution to hadronic EDMs. As mentioned in Sect. 2.2, this is not the only $\not{P}\not{T}$ operator induced at the electroweak scale. The (C)EDM operators of light quarks are also generated, but only through loop diagrams which suppresses the EDMs and CEDMs d_q and $\tilde{d}_q$. In addition, the light-quark EDMs and CEDMs are proportional to a small quark mass, which further suppresses their contribution to hadronic EDMs with respect to the four-quark operators arising from Eq. (8) [69, 70]. The Weinberg three-gluon operator can be produced as well, but only at the two-loop level and its contribution to EDMs is negligible [69, 70]. Finally, $\not{P}\not{T}$ four-quark operators are induced by tree-level exchange of the additional, non-SM-like Higgs particles of the model that have *CP*-violating couplings to quarks. However, the four-quark operators involving light quarks are suppressed by small Yukawa couplings. In combination with the fact that the additional Higgs bosons giving rise to these four-quark operators should be heavy, with masses exceeding 15 TeV in order to evade FCNC constraints [60], we can neglect such four-quark operators [69, 70].

Thus, for hadronic EDMs the most important interaction is the right-handed current interaction in Eq. (8), which is produced after integrating out the $W_R^\pm$ boson. This operator arises from the interaction between the charged gauge-bosons, $W_{L,R}^\pm$, and the bidoublet ϕ defined in Eq. (5). In fact, it is the kinetic term of the bidoublet which is responsible for the mixing between the $W_L^\pm$ and $W_R^\pm$ bosons, which in turn gives rise to the operator in Eq. (8). Using that

$$\mathcal{D}_\mu\phi = \partial_\mu\phi + i\frac{g_L}{2}W_{L\mu}^a\tau^a\phi - i\frac{g_R}{2}\phi W_{R\mu}^a\tau^a \ , \tag{68}$$

where $g_{L,R}$ are the coupling constants of the $SU(2)_{L,R}$ gauge groups which are equal in the mLRSM, $g_L = g_R$, the kinetic term of the bidoublet is given by

$$\mathcal{L} = \mathrm{Tr}[(\mathcal{D}_\mu\phi)^\dagger(\mathcal{D}^\mu\phi)] = \frac{ig_R}{\sqrt{2}}\mathrm{Tr}\left[\begin{pmatrix} 0 & W_{R\mu}^+ \\ W_{R\mu}^- & 0 \end{pmatrix}\phi^\dagger\mathcal{D}^\mu\phi\right] + \text{h.c.} + \dots \ . \tag{69}$$

Here we only kept terms bilinear in $W_R^\pm$. We can now integrate out $W_R^\pm$ to obtain

$$\mathcal{L}_{W_R} = \frac{ig_R^2}{2M_R^2}\mathrm{Tr}\left[\begin{pmatrix} 0 & J_{R\mu}^+ \\ J_{R\mu}^- & 0 \end{pmatrix}\phi^\dagger D_L^\mu\phi\right] + \text{h.c.} + \dots \ , \tag{70}$$

with $J_{R\mu}^- = \overline{U}_R V_R\gamma_\mu D_R$ and $J_{R\mu}^+ = (J_{R\mu}^-)^\dagger$, while V_R is the quark mixing matrix of the right-handed sector, and $M_R \approx g_R v_R$ is the mass of $W_R^\pm$. Moreover,

$$D_L^\mu\phi = \partial^\mu\phi + i\frac{g_L}{2}W_L^{a\mu}\tau^a\phi \ . \tag{71}$$

The form of the interaction in Eq. (8) is already visible in Eq. (70). It only remains to integrate out the heavy Higgs fields. To do so we write the bidoublet ϕ in terms of two $SU(2)_L$ doublets,

$$\phi = (\phi_1, \phi_2) \ , \qquad \phi_1 \equiv \begin{pmatrix} \phi_1^0 \\ \phi_1^- \end{pmatrix} \ , \qquad \phi_2 \equiv \begin{pmatrix} \phi_2^+ \\ \phi_2^0 \end{pmatrix} \ .$$

Since the field φ that corresponds to the SM Higgs field is a doublet under $SU(2)_L$ as well, it is taken to be a linear combination of these fields. The remaining linear combination then only involves Higgs fields that are, by assumption, heavy. To good approximation these Higgs fields are given, in terms of the fields in the mass basis, by [60]:

$$\varphi = \begin{pmatrix} -G_L^+ \\ (h^0 + iG_Z^0)/\sqrt{2} \end{pmatrix} \ , \qquad \varphi_H = \begin{pmatrix} H_2^+ \\ (H_1^0 + iA_1^0)/\sqrt{2} \end{pmatrix} \ . \tag{72}$$

Here G_L^+ and G_Z^0 are the would-be Goldstone boson fields that get absorbed by the W_L^+ and Z_L fields, respectively, while h^0 corresponds to the SM Higgs boson. The fields appearing in φ_H are assumed to be heavy. The basis transformation between the fields $\phi_{1,2}$ and those of Eq. (72) is given by [60]

$$\begin{pmatrix} \varphi \\ \varphi_H \end{pmatrix} = \frac{1}{\sqrt{1+\xi^2}} \begin{pmatrix} -1 & \xi e^{-i\alpha} \\ \xi e^{i\alpha} & 1 \end{pmatrix} \begin{pmatrix} \tilde{\phi}_1 \\ \phi_2 \end{pmatrix} \ , \tag{73}$$

where $\xi = \kappa'/\kappa$ and $\tilde{\phi} = i\tau_2\phi^*$. With Eq. (6) we can check that $\langle\varphi\rangle = \sqrt{\kappa^2 + \kappa'^2} = v/\sqrt{2}$ while $\langle\varphi_H\rangle = 0$.

Using Eq. (73) to rewrite Eq. (69) in terms of the fields in the mass basis and keeping only terms containing the light fields φ, we obtain

$$\begin{aligned} \mathcal{L}_{W_R} &= \frac{ig_R^2}{2M_R^2}\frac{1}{1+\xi^2}\mathrm{Tr}\left[\begin{pmatrix} J_{R\mu}^+ \xi e^{-i\alpha}\varphi^\dagger \\ J_{R\mu}^- \tilde{\varphi}^\dagger \end{pmatrix} D^\mu(\tilde{\varphi},\, \xi e^{i\alpha}\varphi)\right] + \text{h.c.} + \ldots \\ &= \frac{ig_R^2}{2M_R^2}\frac{\xi}{1+\xi^2}\left[e^{i\alpha}\tilde{\varphi}^\dagger(D^\mu\varphi)J_{R\mu}^- + e^{-i\alpha}\varphi^\dagger(D^\mu\tilde{\varphi})J_{R\mu}^+\right] + \text{h.c.} + \ldots \\ &= \frac{ig_R^2}{M_R^2}\frac{\xi}{1+\xi^2}e^{i\alpha}\tilde{\varphi}^\dagger(D^\mu\varphi)J_{R\mu}^- + \text{h.c.} + \ldots \ , \end{aligned} \tag{74}$$

where we used $\left[i\tilde{\varphi}^\dagger(D_\mu\varphi)\right]^\dagger = i\varphi^\dagger(D_\mu\tilde{\varphi})$. Finally, a comparison with Eq. (8) shows that

$$\Xi_1 = \frac{g_R^2}{M_R^2}\frac{\xi}{1+\xi^2}e^{i\alpha}V_R^{ud} \simeq \frac{1}{\kappa^2+\kappa'^2}\frac{\kappa\kappa'}{v_R^2}e^{i\alpha}V_R^{ud} \simeq -\frac{2}{v^2}\sin\zeta\, V_R^{ud}e^{i\alpha} \ . \tag{75}$$

B The aligned two-Higgs doublet model

In this appendix we discuss how the low-energy $\not{P}T$ Lagrangian in Eq. (21) comes about in the a2HDM with the parameter specifications in Eq. (20).

B.1 *CP*-violating four-quark operators

CP-violating four-quark operators with net flavor number zero are induced, in the model with the parameters in Eq. (20), already at tree level by the exchange of the neutral Higgs bosons H and A and of charged Higgs bosons $H^\pm$ with Yukawa interactions in Eq. (16). Because we assume H and A to be (nearly) mass-degenerate, $M_H \simeq M_A \simeq M$, the relation Eq. (19) can be applied to the computation of the coefficients of these operators. Then, as already briefly mentioned in Sect. 2.3, the exchange of H and A induces operators of the type $(\bar{u}u)(\bar{d}i\gamma_5 d)$ and $(\bar{d}d)(\bar{u}i\gamma_5 u)$ with coefficients $\pm m_u m_d \mathrm{Im}(\varsigma_u^* \varsigma_d)/(v^2 M^2)$, where u (d) denotes here any of the up-type (down-type) quarks. The operators that involve light quarks only are severely suppressed by the factor $m_u m_d/v^2$. The contribution of these operators to the EDM of a nucleon turns out to be, after the assumptions in Eq. (20), significantly smaller than the two-loop dipole contributions discussed below in the appendices B.2 and B.3.

The tree-level exchange of the charged Higgs bosons $H^\pm$ between quarks, with Yukawa interactions given in Eq. (16), induces at tree-level the $\not{P}\not{T}$ operators $(\bar{u}d)(\bar{d}i\gamma_5 u)$ and $(\bar{u}i\gamma_5 d)(\bar{d}u)$ with coefficients $2m_u m_d |V_{ud}|^2 \mathrm{Im}(\varsigma_u^* \varsigma_d)/(v^2 M_+^2)$. The above statements on the size of the four-quark contributions induced by neutral Higgs boson exchanges apply also here.

The operators containing heavy quarks can (partially) overcome these suppression factors. However, these operators do not contribute directly to nucleon EDMs. Operators with two heavy quark fields can, after integrating out the heavy quarks, induce dimension-seven operators of the form $(\bar{q}q)\epsilon^{\alpha\beta\mu\nu} G^a_{\alpha\beta} G^a_{\mu\nu}$ and $(\bar{q}i\gamma_5 q) G^a_{\mu\nu} G^{a\,\mu\nu}$ [107, 165], where q denotes a light quark. The size of the contributions of these operators to the nucleon EDM has been estimated in Ref. [107] and also turns out to be significantly smaller than the contributions coming from the two-loop dipole diagrams to be discussed below.

These considerations justify that we neglect the contributions of four-quark operators to the low-energy effective Lagrangian in Eq. (21) in the a2HDM model with the parameter specifications in Eq. (20).

The exchange of the neutral Higgs bosons H and A between quarks and leptons ℓ induces *CP*-violating semileptonic four-fermion operators $(\bar{q}q)(\bar{\ell}i\gamma_5 \ell)$ (and $q \leftrightarrow \ell$) with coefficients $\pm m_q m_\ell \mathrm{Im}(\varsigma_q^* \varsigma_\ell)/(v^2 M^2)$. These are of potential importance for T-violating effects in paramagnetic atoms (*cf.* Sect. 5.1). However, if

$$\mathrm{Im}(\varsigma_q^* \varsigma_\ell) = \mathcal{O}\left(\mathrm{Im}(\varsigma_u^* \varsigma_d)\right) , \tag{76}$$

then the electron EDM induced by two-loop Barr-Zee diagrams [86] dominates by far the contribution to the T-violating effect in the ThO molecule that was recently searched for in Ref. [15].

B.2 Contributions to the quark EDMs and chromo-EDMs

In general, *CP*-violating flavor-diagonal neutral Higgs boson exchanges induce quark (C)EDMs already at one-loop. Because these one-loop terms scale with the third power of the quark mass (modulo logs), $d_q^{(1l)}, \tilde{d}_q^{(1l)} \sim m_q^3/(v^2 M^2)$, they are, in the case of light quarks, suppressed as compared to the two-loop Barr-Zee contributions. Although these are nominally suppressed by an additional loop factor $\alpha/(4\pi)$, respectively $\alpha_s/(4\pi)$, where α (α_s) is the QED (QCD) coupling, they involve only one power (modulo logs) of m_q. In the a2HDM with the specifications of Eq. (20), the one-loop exchanges of the neutral Higgs bosons H and A cannot, in fact, generate a one-loop contribution to a quark (C)EDM. This follows from Eq. (19). The exchange of a

charged Higgs boson does generate a one-loop contribution. For instance, the EDM of the d quark receives a contribution $d_q^{(1l)}(H^+) \sim 2m_d m_u^2 |V_{ud}|^2 \mathrm{Im}(\varsigma_u^* \varsigma_d)/(v^2 M_+^2)$. But also these one-loop terms are subdominant compared to the two-loop terms that we now discuss and can therefore be neglected.

For the general a2HDM with the Yukawa interactions of Eq. (16) and the couplings in Eqs. (17) and (18) the Barr-Zee-type diagrams involving a *CP*-violating neutral spin-zero particle and a quark in the loop induce the following contribution to the quark EDM and CEDM, respectively [62, 86, 166, 167]:

$$\begin{aligned} d_q(\mu_H; \varphi^0, q) &= 24 e Q_q m_q \frac{\alpha}{(4\pi)^3 v^2} \sum_{q',i} Q_{q'}^2 \left[f\left(\frac{m_{q'}^2}{M_i^2}\right) \mathrm{Re}\, y_q^i \mathrm{Im}\, y_{q'}^i + g\left(\frac{m_{q'}^2}{M_i^2}\right) \mathrm{Re}\, y_{q'}^i \mathrm{Im}\, y_q^i \right] , \\ \tilde{d}_q(\mu_H; \varphi^0, q) &= -4 m_q \frac{g_s \alpha_s}{(4\pi)^3 v^2} \sum_{q',i} \left[f\left(\frac{m_{q'}^2}{M_i^2}\right) \mathrm{Re}\, y_q^i \mathrm{Im}\, y_{q'}^i + g\left(\frac{m_{q'}^2}{M_i^2}\right) \mathrm{Re}\, y_{q'}^i \mathrm{Im}\, y_q^i \right] , \end{aligned} \tag{77}$$

where $e > 0$, $Q_u = 2/3, Q_d = -1/3$, and the label μ_H indicates that these are the quark (C)EDMs at a scale $\mu_H \sim m_t \sim M_\varphi$. The QCD coupling is understood to be evaluated at the scale μ_H. For a neutral spin-zero particle and a $W^\pm$ boson in the loop one gets [62, 86, 166, 167]:

$$d_q(\mu_H; \varphi^0, W^\pm) = -4 e Q_q m_q \frac{\alpha}{(4\pi)^3 v^2} \sum_i \left[3 f\left(\frac{M_W^2}{M_i^2}\right) + 5 g\left(\frac{M_W^2}{M_i^2}\right) \right] \mathrm{Im}\left(y_q^i R_{i1}\right) , \tag{78}$$

where

$$f(z) \equiv \frac{z}{2} \int_0^1 dx \frac{1-2x(1-x)}{x(1-x)-z} \ln \frac{x(1-x)}{z} , \qquad g(z) \equiv \frac{z}{2} \int_0^1 dx \frac{1}{x(1-x)-z} \ln \frac{x(1-x)}{z} . \tag{79}$$

We now apply the specifications of Eq. (20). Then the contribution in Eq. (78) is zero, because $R_{11} = 1$, $R_{21} = R_{23} = 0$ and $y_q^1 = 1$. Eqs. (20) and (19) imply that up-type quarks in the fermion loop contribute only to the (C)EDM of a down-type quark and vice versa. Therefore, diagrams with a top quark in the loop contribute only to the (C)EDM of the d quark. Diagrams with quarks $q \neq t$ in the loop are suppressed by at least roughly two orders of magnitude as compared to the t-quark contribution, because of smaller Yukawa couplings. (This is reflected in the significantly smaller magnitudes of the respective values of the functions f and g.) Therefore, in the a2HDM with the assumptions in Eq. (20), the EDM and CEDM of the u quark in the low-energy effective Lagrangian can be neglected as compared to those of the d quark. There are also contributions to d_q from charged leptons in the fermion loop but, assuming that the relation in Eq. (76) holds, these can also be neglected as compared to the t-quark contribution to d_d.

Another set of Barr-Zee type contributions to d_q involves charged Higgs boson exchange [62, 167, 168]. They contribute significantly to the d-quark EDM only, while the u-quark EDM is again negligible [62, 167]:

$$d_d(\mu_H; H^\pm) = m_d \frac{12 M_W^2}{(4\pi v)^4} |V_{tb}|^2 |V_{ud}|^2 \mathrm{Im}\left(\varsigma_u^* \varsigma_d\right) (e Q_t F_t + e Q_b F_b) , \tag{80}$$

where

$$F_q = \frac{T_q(z_{H^\pm}) - T_q(z_W)}{z_{H^\pm} - z_W} , \qquad z_i \equiv \frac{M_i^2}{m_t^2} , \tag{81}$$

and

$$T_t(z) = \frac{1-3z}{z^2}\frac{\pi^2}{6} + \left(\frac{1}{z}-\frac{5}{2}\right)\ln z - \frac{1}{z} - \left(2-\frac{1}{z}\right)\left(1-\frac{1}{z}\right)\mathrm{Li}_2(1-z) \ ,$$
$$T_b(z) = \frac{2z-1}{z^2}\frac{\pi^2}{6} + \left(\frac{3}{2}-\frac{1}{z}\right)\ln z + \frac{1}{z} - \frac{1}{z}\left(2-\frac{1}{z}\right)\mathrm{Li}_2(1-z) \ . \quad (82)$$

This contribution to d_d is not affected by the parameter choices in Eq. (20).

Additionally, there are contributions to the quark EDMs through diagrams which are similar to those that gave rise to Eq. (80), but where the virtual quark loop is replaced by a loop involving the spin-zero fields [82, 167]. These diagrams are proportional to a different *CP*-violating parameter than the one encountered so far. Although these diagrams generate u- and d-quark EDMs of similar size, the contributions from these diagrams are smaller by a factor of a few than the ones in Eqs. (77), see Ref. [167]. In addition, they do not contribute to the quark CEDMs which play the dominant role in our analysis. Thus, under the assumption that the *CP*-violation parameters are of similar magnitude, these diagrams are expected to be less important than the CEDMs. Therefore, we neglect them in our analysis.

In summary, we obtain in the a2HDM with the parameter specifications in Eq. (20) that at a high scale μ_H the d-quark (C)EDM is significantly larger than the corresponding dipole moment of the u quark. The d-quark EDM and CEDM are given by, putting $\mu_H = m_t$:

$$d_d(m_t) = e\frac{Q_d m_d \alpha}{(4\pi)^3 v^2}\mathrm{Im}\left(\varsigma_u^*\varsigma_d\right)\left(\frac{32}{3}\left[f\left(\frac{m_t^2}{M^2}\right)+g\left(\frac{m_t^2}{M^2}\right)\right] + \frac{3}{s_w^2}|V_{ud}|^2|V_{tb}|^2\left[F_b - 2F_t\right]\right), \quad (83)$$
$$\tilde{d}_d(m_t) = -4m_d\frac{g_s\alpha_s}{(4\pi)^3 v^2}\mathrm{Im}\left(\varsigma_u^*\varsigma_d\right)\left[f\left(\frac{m_t^2}{M^2}\right)+g\left(\frac{m_t^2}{M^2}\right)\right] \ . \quad (84)$$

They depend on a common unknown factor $\mathrm{Im}\left(\varsigma_u^*\varsigma_d\right)$ that signifies non-KM *CP* violation of the model. By renormalization-group evolution down to the scale $\mu = \Lambda_\chi$ we obtain the d-quark (C)EDM given in Eqs. (21) and (22).

B.3 Contributions to the Weinberg operator

The leading-order contributions to the Weinberg operator corresponds to diagrams of the type shown in Fig. 2(c). From diagrams that involve *CP*-violating flavor-diagonal neutral Higgs boson exchange the coefficient of the Weinberg operator, i.e., the CEDM of the gluon, receives, in the 2HDM, the following contribution [29, 62, 169]:

$$d_W(m_t;\varphi^0) = -\frac{4g_s^3}{(4\pi)^4 v^2}\sum_{q,i}\mathrm{Re}\, y_q^i \mathrm{Im}\, y_q^i\, h(m_q,\, M_i) \ , \quad (85)$$

where

$$h(m,M) = \frac{m^4}{4}\int_0^1 dx \int_0^1 du \frac{u^3x^3(1-x)}{[m^2x(1-ux)+M^2(1-u)(1-x)]^2} \ . \quad (86)$$

As we restrict ourselves to the parameters of Eq. (20), this contribution will be proportional to $\mathrm{Im}(\varsigma_q^*\varsigma_q)$ and therefore vanishes.

The exchange of a charged Higgs boson with Yukawa couplings given in Eq. (21) leads to diagrams similar to Fig. 2(c). In this case both a bottom and top quark are present in the fermion

loop. The amplitude involves two different scales, $M_+ \sim m_t$, and m_b. One may evaluate it in the framework of effective field theory[25] [25, 62, 170]. One can first integrate out the charged Higgs boson and the top quark. This generates a one-loop contribution to the bottom quark CEDM. At the bottom quark threshold this b-quark CEDM then induces a one-loop contribution [25] to d_W. The first step gives [62, 169, 170]:

$$\tilde{d}_b(m_t; H^\pm) = -\frac{g_s(m_t)}{8\pi^2 v^2} m_b(m_t) |V_{tb}|^2 \mathrm{Im}\,(\varsigma_d \varsigma_u^*) \left[x_t \left(\frac{\ln x_t}{(x_t-1)^3} + \frac{x_t - 3}{2(x_t-1)^2} \right) \right] \ , \tag{87}$$

where $x_t = m_t^2/M_+^2$ and $m_b(m_t)$ is the $\overline{\mathrm{MS}}$ mass of the b quark at the scale $\mu = m_t$. At $\mu = m_b$ this induces a contribution to the Weinberg operator [25],

$$d_W(m_b; H^\pm) = -\frac{g_s^2(m_b)}{32\pi^2 m_b(m_b)} \tilde{d}_b(m_b; H^\pm) \ , \tag{88}$$

where $m_b(m_b)$ denotes the $\overline{\mathrm{MS}}$ mass at $\mu = m_b$ and $\tilde{d}_b(m_b; H^\pm)$ is related to $\tilde{d}_b(m_t; H^\pm)$ by a renormalization-group factor: $\tilde{d}_b(m_b; H^\pm) = \eta'_W \tilde{d}_b(m_t; H^\pm)$ where we introduced the parameter $\eta'_W = \left(\frac{\alpha_s(m_t)}{\alpha_s(m_b)}\right)^{-19/46} \simeq 1.3$ [24–28].

In summary, we obtain in the a2HDM with the parameter set of Eq. (20) the following CEDM d_W of the gluon at the scale $\mu = m_b$:

$$d_W(m_b) \ = \ \eta_W \frac{g_s \alpha_s}{(4\pi)^3 v^2} |V_{tb}|^2 \mathrm{Im}\,(\varsigma_u^* \varsigma_d) \left[x_t \left(\frac{\ln x_t}{(x_t-1)^3} + \frac{x_t - 3}{2(x_t-1)^2} \right) \right] \ , \tag{89}$$

where the factors of g_s and α_s are to be evaluated at the scale $\mu = m_b$ while the parameter $\eta_W = \frac{g_s(m_t)}{g_s(m_b)} \frac{m_b(m_t)}{m_b(m_b)} \eta'_W = \left(\frac{\alpha_s(m_t)}{\alpha_s(m_b)}\right)^{14/23} \simeq 0.67$ is the resulting renormalization-group factor due to the evolution from the scale m_t to m_b. The renormalization-group evolution of Eq. (89) to the scale $\mu = \Lambda_\chi$ then yields $d_W(\Lambda_\chi)$ given in Eqs. (21) and (22).

[25] Alternatively, this two-loop amplitude was computed directly in Ref. [169]. This result can then by renormalization-group evolution be evaluated at a low scale.

References

[1] N. Cabibbo, Phys. Rev. Lett. **10**, 531 (1963).

[2] M. Kobayashi and T. Maskawa, Prog. Theor. Phys. **49**, 652 (1973).

[3] G. 't Hooft, Phys. Rev. Lett. **37**, 8 (1976).

[4] G. 't Hooft, Phys. Rev. D **14**, 3432 (1976).

[5] C. A. Baker *et al.*, Phys. Rev. Lett. **97**, 131801 (2006), hep-ex/0602020.

[6] V. Baluni, Phys. Rev. D **19**, 2227 (1979).

[7] R. J. Crewther, P. Di Vecchia, G. Veneziano, and E. Witten, Phys. Lett. B **88**, 123 (1979).

[8] A. Riotto and M. Trodden, Ann. Rev. Nucl. Part. Sci. **49**, 35 (1999), hep-ph/9901362.

[9] V. A. Kuzmin, M. E. Shaposhnikov, and I. I. Tkachev, Phys. Rev. D **45**, 466 (1992).

[10] I. B. Khriplovich and S. K. Lamoreaux, CP violation without strangeness: Electric dipole moments of particles, atoms, and molecules, Springer Verlag (1997).

[11] M. Pospelov and A. Ritz, Annals Phys. **318**, 119 (2005), hep-ph/0504231.

[12] J. Engel, M. J. Ramsey-Musolf, and U. van Kolck, Prog. Part. Nucl. Phys. **71**, 21 (2013), 1303.2371.

[13] J. L. Hewett *et al.*, (2012), 1205.2671.

[14] W. C. Griffith *et al.*, Phys. Rev. Lett. **102**, 101601 (2009).

[15] ACME Collaboration, J. Baron *et al.*, Science **343**, 269 (2014), 1310.7534.

[16] F. J. M. Farley *et al.*, Phys. Rev. Lett. **93**, 052001 (2004), hep-ex/0307006.

[17] C. J. G. Onderwater, J. Phys. Conf. Ser. **295**, 012008 (2011).

[18] J. Pretz, Hyperfine Interact. **214**, 111 (2013), 1301.2937.

[19] JEDI-collaboration, http://collaborations.fz-juelich.de/ikp/jedi/ .

[20] A. Czarnecki and B. Krause, Phys.Rev.Lett. **78**, 4339 (1997), hep-ph/9704355.

[21] T. Mannel and N. Uraltsev, Phys.Rev. **D85**, 096002 (2012), 1202.6270.

[22] W. Buchmüller and D. Wyler, Nucl. Phys. B **268**, 621 (1986).

[23] B. Grzadkowski, M. Iskrzynski, M. Misiak, and J. Rosiek, JHEP **1010**, 085 (2010), 1008.4884.

[24] F. Wilczek and A. Zee, Phys. Rev. D **15**, 2660 (1977).

[25] E. Braaten, C.-S. Li, and T.-C. Yuan, Phys. Rev. Lett. **64**, 1709 (1990).

[26] G. Degrassi, E. Franco, S. Marchetti, and L. Silvestrini, JHEP **0511**, 044 (2005), hep-ph/0510137.

[27] J. Hisano, K. Tsumura, and M. J. S. Yang, Phys. Lett. B **713**, 473 (2012), 1205.2212.

[28] W. Dekens and J. de Vries, JHEP **1305**, 149 (2013), 1303.3156.

[29] S. Weinberg, Phys. Rev. Lett. **63**, 2333 (1989).

[30] E. Braaten, C. S. Li, and T. C. Yuan, Phys. Rev. D **42**, 276 (1990).

[31] S. Weinberg, Physica **A96**, 327 (1979).

[32] J. Gasser and H. Leutwyler, Annals Phys. **158**, 142 (1984).

[33] J. Gasser, M. E. Sainio, and A. Svarć, Nucl. Phys. B **307**, 779 (1988).

[34] S. Weinberg, The Quantum Theory of Fields, Vol. 2, Cambridge University Press (1996).

[35] V. Bernard, N. Kaiser, and U.-G. Meißner, Int. J. Mod. Phys. E **4**, 193 (1995), hep-ph/9501384.

[36] P. F. Bedaque and U. van Kolck, Ann. Rev. Nucl. Part. Sci. **52**, 339 (2002), nucl-th/0203055.

[37] E. Epelbaum, H.-W. Hammer, and U.-G. Meißner, Rev. Mod. Phys. **81**, 1773 (2009), 0811.1338.

[38] R. Machleidt and D. R. Entem, Phys. Rept. **503**, 1 (2011), 1105.2919.

[39] E. Mereghetti, W. Hockings, and U. van Kolck, Annals Phys. **325**, 2363 (2010), 1002.2391.

[40] J. de Vries, E. Mereghetti, R. G. E. Timmermans, and U. van Kolck, Annals Phys. **338**, 50 (2013), 1212.0990.

[41] A. Pich and E. de Rafael, Nucl. Phys. B **367**, 313 (1991).

[42] B. Borasoy, Phys. Rev. D **61**, 114017 (2000), hep-ph/0004011.

[43] W. H. Hockings and U. van Kolck, Phys. Lett. B **605**, 273 (2005), nucl-th/0508012.

[44] S. Narison, Phys. Lett. B **666**, 455 (2008), 0806.2618.

[45] K. Ottnad, B. Kubis, U.-G. Meißner, and F.-K. Guo, Phys. Lett. B **687**, 42 (2010), 0911.3981.

[46] J. de Vries, R. G. E. Timmermans, E. Mereghetti, and U. van Kolck, Phys. Lett. B **695**, 268 (2011), 1006.2304.

[47] E. Mereghetti, J. de Vries, W. H. Hockings, C. M. Maekawa, and U. van Kolck, Phys. Lett. B **696**, 97 (2011), 1010.4078.

[48] F.-K. Guo and U.-G. Meißner, JHEP **1212**, 097 (2012), 1210.5887.

[49] J. de Vries, E. Mereghetti, R. G. E. Timmermans, and U. van Kolck, Phys. Rev. Lett. **107**, 091804 (2011), 1102.4068.

[50] J. de Vries *et al.*, Phys. Rev. C **84**, 065501 (2011), 1109.3604.

[51] J. Bsaisou *et al.*, Eur. Phys. J. A **49**, 31 (2013), 1209.6306.

[52] J. H. de Jesus and J. Engel, Phys. Rev. C **72**, 045503 (2005), nucl-th/0507031.

[53] O. Lebedev, K. A. Olive, M. Pospelov, and A. Ritz, Phys. Rev. D **70**, 016003 (2004), hep-ph/0402023.

[54] J. Bsaisou, Ph.D. Thesis, University of Bonn (2014).

[55] J. Bsaisou *et al.*, In preparation (2014).

[56] R. D. Peccei and H. R. Quinn, Phys. Rev. Lett. **38**, 1440 (1977).

[57] R. Peccei and H. R. Quinn, Phys. Rev. D **16**, 1791 (1977).

[58] J. C. Pati and A. Salam, Phys. Rev. D **10**, 275 (1974).

[59] R. N. Mohapatra and J. C. Pati, Phys. Rev. D **11**, 566 (1975).

[60] Y. Zhang, H. An, X. Ji, and R. N. Mohapatra, Nucl. Phys. B **802**, 247 (2008), 0712.4218.

[61] A. Pich and P. Tuzon, Phys. Rev. D **80**, 091702 (2009), 0908.1554.

[62] M. Jung and A. Pich, (2013), 1308.6283.

[63] Particle Data Group, J. Beringer *et al.*, Phys. Rev. D **86**, 010001 (2012).

[64] G. Senjanovic and R. N. Mohapatra, Phys. Rev. D **12**, 1502 (1975).

[65] G. Senjanovic, Nucl. Phys. B **153**, 334 (1979).

[66] N. G. Deshpande, J. F. Gunion, B. Kayser, and F. I. Olness, Phys. Rev. D **44**, 837 (1991).

[67] S. Bertolini, A. Maiezza, and F. Nesti, (2014), 1403.7112.

[68] A. Maiezza, M. Nemevsek, F. Nesti, and G. Senjanovic, Phys. Rev. D **82**, 055022 (2010), 1005.5160.

[69] F. Xu, H. An, and X. Ji, JHEP **1003**, 088 (2010), 0910.2265.

[70] H. An, X. Ji, and F. Xu, JHEP **1002**, 043 (2010), 0908.2420.

[71] J. Ng and S. Tulin, Phys. Rev. D **85**, 033001 (2012), 1111.0649.

[72] ATLAS Collaboration, G. Aad *et al.*, Phys.Lett. **B716**, 1 (2012), 1207.7214.

[73] CMS Collaboration, S. Chatrchyan *et al.*, Phys.Lett. **B716**, 30 (2012), 1207.7235.

[74] C.-Y. Seng, J. de Vries, E. Mereghetti, H. H. Patel, and M. Ramsey-Musolf, (2014), 1401.5366.

[75] J. F. Gunion, H. E. Haber, G. L. Kane, and S. Dawson, The Higgs Hunter's Guide, Perseus Publishing (1990).

[76] I. I. Bigi and A. Sanda, CP violation (Second edition), Cambridge University Press (2009).

[77] G. Branco *et al.*, Phys. Rept. **516**, 1 (2012), 1106.0034.

[78] G. D'Ambrosio, G. Giudice, G. Isidori, and A. Strumia, Nucl.Phys. **B645**, 155 (2002), hep-ph/0207036.

[79] A. Buras, P. Gambino, M. Gorbahn, S. Jager, and L. Silvestrini, Phys.Lett. **B500**, 161 (2001), hep-ph/0007085.

[80] A. J. Buras, G. Isidori, and P. Paradisi, Phys.Lett. **B694**, 402 (2011), 1007.5291.

[81] W. Bernreuther, T. Schroder, and T. Pham, Phys.Lett. **B279**, 389 (1992).

[82] S. Inoue, M. J. Ramsey-Musolf, and Y. Zhang, (2014), 1403.4257.

[83] ATLAS, CMS Collaboration, M. P. Sanders, PoS **DIS2013**, 010 (2013).

[84] CMS Collaboration, S. Meola, PoS **DIS2013**, 093 (2013).

[85] K. Cheung, J. S. Lee, E. Senaha, and P.-Y. Tseng, (2014), 1403.4775.

[86] S. M. Barr and A. Zee, Phys. Rev. Lett. **65**, 21 (1990).

[87] T. Ibrahim and P. Nath, Rev.Mod.Phys. **80**, 577 (2008), 0705.2008.

[88] J. R. Ellis, S. Ferrara, and D. V. Nanopoulos, Phys.Lett. **B114**, 231 (1982).

[89] W. Buchmuller and D. Wyler, Phys.Lett. **B121**, 321 (1983).

[90] J. Polchinski and M. B. Wise, Phys.Lett. **B125**, 393 (1983).

[91] F. del Aguila, M. Gavela, J. Grifols, and A. Mendez, Phys.Lett. **B126**, 71 (1983).

[92] J. Dai, H. Dykstra, R. Leigh, S. Paban, and D. Dicus, Phys.Lett. **B237**, 216 (1990).

[93] O. Lebedev and M. Pospelov, Phys.Rev.Lett. **89**, 101801 (2002), hep-ph/0204359.

[94] A. Pilaftsis, Phys.Lett. **B435**, 88 (1998), hep-ph/9805373.

[95] D. Chang, W.-Y. Keung, and A. Pilaftsis, Phys.Rev.Lett. **82**, 900 (1999), hep-ph/9811202.

[96] D. Chang, W.-F. Chang, and W.-Y. Keung, Phys.Lett. **B478**, 239 (2000), hep-ph/9910465.

[97] A. Pilaftsis, Nucl.Phys. **B644**, 263 (2002), hep-ph/0207277.

[98] M. S. Carena, J. R. Ellis, A. Pilaftsis, and C. Wagner, Phys.Lett. **B495**, 155 (2000), hep-ph/0009212.

[99] A. Pilaftsis, Phys.Rev. **D62**, 016007 (2000), hep-ph/9912253.

[100] N. Yamanaka, Phys.Rev. **D87**, 011701 (2013), 1211.1808.

[101] Y. Kizukuri and N. Oshimo, Phys.Rev. **D46**, 3025 (1992).

[102] T. Ibrahim and P. Nath, Phys.Rev. **D58**, 111301 (1998), hep-ph/9807501.

[103] M. Brhlik, G. J. Good, and G. L. Kane, Phys.Rev. **D59**, 115004 (1999), hep-ph/9810457.

[104] A. Bartl, T. Gajdosik, W. Porod, P. Stockinger, and H. Stremnitzer, Phys.Rev. **D60**, 073003 (1999), hep-ph/9903402.

[105] S. Abel, D. Bailin, S. Khalil, and O. Lebedev, Phys.Lett. **B504**, 241 (2001), hep-ph/0012145.

[106] S. Abel, S. Khalil, and O. Lebedev, Nucl.Phys. **B606**, 151 (2001), hep-ph/0103320.

[107] D. A. Demir, O. Lebedev, K. A. Olive, M. Pospelov, and A. Ritz, Nucl. Phys. B **680**, 339 (2004), hep-ph/0311314.

[108] N. Arkani-Hamed, S. Dimopoulos, G. Giudice, and A. Romanino, Nucl.Phys. **B709**, 3 (2005), hep-ph/0409232.

[109] S. Abel and O. Lebedev, JHEP **0601**, 133 (2006), hep-ph/0508135.

[110] D. Chang, W.-F. Chang, and W.-Y. Keung, Phys.Rev. **D71**, 076006 (2005), hep-ph/0503055.

[111] G. Giudice and A. Romanino, Phys.Lett. **B634**, 307 (2006), hep-ph/0510197.

[112] J. Hisano, M. Nagai, and P. Paradisi, Phys.Lett. **B642**, 510 (2006), hep-ph/0606322.

[113] S. Yaser Ayazi and Y. Farzan, Phys.Rev. **D74**, 055008 (2006), hep-ph/0605272.

[114] J. R. Ellis, J. S. Lee, and A. Pilaftsis, JHEP **0810**, 049 (2008), 0808.1819.

[115] Y. Li, S. Profumo, and M. Ramsey-Musolf, JHEP **1008**, 062 (2010), 1006.1440.

[116] J. Ellis, J. S. Lee, and A. Pilaftsis, JHEP **1102**, 045 (2011), 1101.3529.

[117] K. Fuyuto, J. Hisano, N. Nagata, and K. Tsumura, JHEP **1312**, 010 (2013), 1308.6493.

[118] P. Bechtle *et al.*, JHEP **1206**, 098 (2012), 1204.4199.

[119] P. Bechtle *et al.*, (2013), 1310.3045.

[120] J. R. Ellis, J. S. Lee, and A. Pilaftsis, Phys.Rev. **D70**, 075010 (2004), hep-ph/0404167.

[121] J. R. Ellis, J. S. Lee, and A. Pilaftsis, Phys.Rev. **D76**, 115011 (2007), 0708.2079.

[122] A. Manohar and H. Georgi, Nucl. Phys. B **234**, 189 (1984).

[123] N. Fettes, U.-G. Meißner, and S. Steininger, Nucl. Phys. A **640**, 199 (1998), hep-ph/9803266.

[124] J. Gasser and H. Leutwyler, Phys. Rept. **87**, 77 (1982).

[125] A. Walker-Loud, C. E. Carlson, and G. A. Miller, Phys. Rev. Lett. **108**, 232301 (2012), 1203.0254.

[126] V. Baru *et al.*, Nucl. Phys. A **872**, 69 (2011), 1107.5509.

[127] J. Gasser and H. Leutwyler, Nucl. Phys. B **250**, 465 (1985).

[128] N. Fettes, U.-G. Meißner, M. Mojzis, and S. Steininger, Annals Phys. **283**, 273 (2000), hep-ph/0001308.

[129] C. Hanhart and A. Wirzba, Phys. Lett. B **650**, 354 (2007), nucl-th/0703012.

[130] E. Mereghetti, Private communication (2014).

[131] D. A. Demir, M. Pospelov, and A. Ritz, Phys. Rev. D **67**, 015007 (2003), hep-ph/0208257.

[132] M. Pospelov, Phys. Lett. B **530**, 123 (2002), hep-ph/0109044.

[133] M. Pospelov and A. Ritz, Phys. Rev. D **63**, 073015 (2001), hep-ph/0010037.

[134] J. Hisano, J. Y. Lee, N. Nagata, and Y. Shimizu, Phys. Rev. D **85**, 114044 (2012), 1204.2653.

[135] K. Fuyuto, J. Hisano, and N. Nagata, Phys. Rev. D **87**, 054018 (2013), 1211.5228.

[136] C. M. Maekawa, E. Mereghetti, J. de Vries, and U. van Kolck, Nucl. Phys. A **872**, 117 (2011), 1106.6119.

[137] I. B. Khriplovich and R. A. Korkin, Nucl. Phys. A **665**, 365 (2000), nucl-th/9904081.

[138] C.-P. Liu and R. G. E. Timmermans, Phys. Rev. C **70**, 055501 (2004), nucl-th/0408060.

[139] I. R. Afnan and B. F. Gibson, Phys. Rev. C **82**, 064002 (2010), 1011.4968.

[140] Y.-H. Song, R. Lazauskas, and V. Gudkov, Phys.Rev. **C87**, 015501 (2013), 1211.3762.

[141] I. Stetcu, C.-P. Liu, J. L. Friar, A. C. Hayes, and P. Navratil, Phys.Lett. **B665**, 168 (2008), 0804.3815.

[142] Y. Avishai and M. Fabre De La Ripelle, Phys. Rev. Lett. **56**, 2121 (1986).

[143] J. J. Hudson *et al.*, Nature **473**, 493 (2011).

[144] D. M. Kara *et al.*, New J. Phys. **14**, 103051 (2012), 1208.4507.

[145] B. C. Regan, E. D. Commins, C. J. Schmidt, and D. DeMille, Phys. Rev. Lett. **88**, 071805 (2002).

[146] K. Choi and J. Hong, Phys. Lett. B **259**, 340 (1991).

[147] F. Hoogeveen, Nucl.Phys. **B341**, 322 (1990).

[148] M. Pospelov and I. Khriplovich, Sov.J.Nucl.Phys. **53**, 638 (1991).

[149] W. Fischler, S. Paban, and S. D. Thomas, Phys.Lett. **B289**, 373 (1992), hep-ph/9205233.

[150] G. Beall and A. Soni, Phys. Rev. Lett. **47**, 552 (1981).

[151] G. Ecker, W. Grimus, and H. Neufeld, Nucl.Phys. **B229**, 421 (1983).

[152] J. F. Nieves, D. Chang, and P. B. Pal, Phys. Rev. D **33**, 3324 (1986).

[153] M.-C. Chen and K. T. Mahanthappa, Phys. Rev. D **75**, 015001 (2007), hep-ph/0609288.

[154] L. Schiff, Phys.Rev. **132**, 2194 (1963).

[155] V. A. Dzuba, V. V. Flambaum, J. S. M. Ginges, and M. G. Kozlov, Phys. Rev. A **66**, 012111 (2002), hep-ph/0203202.

[156] V. A. Dzuba, V. V. Flambaum, and S. G. Porsev, Phys. Rev. A **80**, 032120 (2009), 0906.5437.

[157] V. A. Dzuba and V. V. Flambaum, Int. J. Mod. Phys. E **21**, 1230010 (2012), 1209.2200.

[158] V. F. Dmitriev and R. A. Sen'kov, Phys. Atom. Nucl. **66**, 1940 (2003), nucl-th/0304048.

[159] S. Ban, J. Dobaczewski, J. Engel, and A. Shukla, Phys. Rev. C **82**, 015501 (2010), 1003.2598.

[160] S. Eidelman *et al.*, Physics Letters B **592**, 1 (2004).

[161] G. Colangelo *et al.*, Eur. Phys. J. C **71**, 1695 (2011), 1011.4408.

[162] S. Aoki *et al.*, (2013), 1310.8555.

[163] S. R. Beane, K. Orginos, and M. J. Savage, Nucl. Phys. B **768**, 38 (2007), hep-lat/0605014.

[164] S. Borsanyi *et al.*, Phys.Rev.Lett. **111**, 252001 (2013), 1306.2287.

[165] A. A. Anselm, V. E. Bunakov, V. P. Gudkov, and N. Uraltsev, Phys. Lett. **B152**, 116 (1985).

[166] J. Gunion and D. Wyler, Phys.Lett. **B248**, 170 (1990).

[167] T. Abe, J. Hisano, T. Kitahara, and K. Tobioka, JHEP **1401**, 106 (2014), 1311.4704.

[168] D. Bowser-Chao, D. Chang, and W.-Y. Keung, Phys.Rev.Lett. **79**, 1988 (1997), hep-ph/9703435.

[169] D. A. Dicus, Phys.Rev. **D41**, 999 (1990).

[170] G. Boyd, A. K. Gupta, S. P. Trivedi, and M. B. Wise, Phys.Lett. **B241**, 584 (1990).